UNCLASSIFIED

AD 400 489

UNCLASSIFIED

63-3-1

ASD-TDR-63-84

APPLIED RESEARCH ON TSEM IMAGE AMPLIFICATION
CAMERA TUBE

TECHNICAL DOCUMENTARY REPORT NO. ASD-TDR-63-84

January 1963

Electronic Technology Laboratory
Aeronautical Systems Division
Air Force Systems Command
Wright-Patterson Air Force Base, Ohio

Project No. 4156, Task No. 415605

(Prepared under Contract No. AF 33(616)-8017
by Westinghouse Electric Company,
Westinghouse Research Laboratories, Pittsburgh, Pa.,
and Electronic Tube Division, Elmira, New York.
Authors : Dr. G. W. Goetze, A. H. Boerio, V. J. Santilli and H. Shabanowitz.)

NOTICES

When Government drawings, specifications, or other data are used for any purpose other than in connection with a definitely related Government procurement operation, the United States Government thereby incurs no responsibility nor any obligation whatsoever; and the fact that the Government may have formulated, furnished, or in any way supplied the said drawings, specifications, or other data, is not to be regarded by implication or otherwise as in any manner licensing the holder or any other person or corporation, or conveying any rights or permission to manufacture, use, or sell any patented invention that may in any way be related thereto.

Qualified requesters may obtain copies of this report from the Armed Services Technical Information Agency, (ASTIA), Arlington Hall Station, Arlington 12, Virginia.

This report has been released to the Office of Technical Services, U.S. Department of Commerce, Washington 25, D.C., for sale to the general public.

Copies of this report should not be returned to the Aeronautical Systems Division unless return is required by security considerations, contractual obligations, or notice on a specific document.

C

FOREWORD

This report was prepared by Dr. G. W. Goetze and Mr. A. H. Boerio, Westinghouse Research Laboratories and Mr. V. J. Santilli and Mr. H. Shabanowitz, Electronic Tube Division, Westinghouse Electric Corporation, on Air Force Contract AF 33(616)-8017, for the Aeronautical Systems Division, Air Force Systems Command. The work reported here, "Applied Research on TSEM Image Amplification Camera Tube", represents the joint effort of the Research Laboratories and the Electronic Tube Division, Westinghouse Electric Corporation, during the period March 1961 - August 1962 on Project 4156, Electronic Tube Technology, under the cognizance of Mr. Melvin R. St. John, Air Force Project Scientist, Electronic Technology Laboratory, Wright-Patterson Air Force Base.

Acknowledgement is made to Messrs. A. E. Anderson, J. A. Hall, W. O. Mansfield, R. A. Shaffer, D. D. Doughty, J. S. Kalafut and Dr. G. Skorinko for their technical and editorial contributions.

ABSTRACT

The concept of minimum detectable contrast is used to describe the capability of an imaging device to discriminate between a signal and the fluctuations of the background. For a given optical system and photocathode illumination, the minimum detectable contrast is reduced by increasing either the integration time, the photo-electron utilization efficiency or both. The maximum integration time is ultimately limited by the electrical storage capacity and the resistivity of the target. The photoelectron utilization efficiency depends on both the total system gain and the statistical fluctuations in gain, especially the gain fluctuations of the first photoelectronic stage. However, gain fluctuations become significant only in those cases where the system gain is approximately equal to or greater than the gain required to see photoelectron scintillations.

The limitations of the TSE intensifier-orthicon, employing transmission secondary electron emission films as pre-scanning beam amplifiers, has been further investigated. Although an appreciable improvement in performance of these tubes was realized during the course of this contract, the theoretically predicted performance was not attained. A fundamental limitation may be the limited resolution realizable in the final TSEM dynode to target stage of the preamplifier section. As a result of these limitations and the concurrent successful development of a low density KCl film, our efforts were directed toward the application of this film as a high gain target in television camera tubes. The low density KCl deposit, which exhibits high gain and high resistivity, depends primarily on free secondary electrons for conduction across the layer. This target has been measured and evaluated with respect to conventional television requirements as well as the requirements of low light level imaging. Experimental data has demonstrated that camera tubes employing this target with direct beam readout have met predicted performance. Furthermore, the theoretically predicted performance of a camera tube employing the high gain target with return beam multiplication, approaches photoelectron noise limited performance.

SECTION 1

INTRODUCTION

An analysis of television camera tube limitations concludes that an advanced
scanned optical amplifier, embodying suitable means of image intensification, is
an effective approach to an ideal imaging tube performance limited only by
statistical fluctuations of the input signal. Various means of intensifying the
image signal electronically have been investigated. At present, there are two
types of image amplifiers which approach the ideal performance levels. They are
the Westinghouse Astracon tube embodying transmission secondary electron emission
dynodes[1] and the cascaded image intensifier tube using phosphor-photocathode
intensifier stages[2]. These devices characteristically approach theoretical
performance very closely for modest resolution, about 1 to 6 line pairs per
millimeter at the tube input. At higher resolutions, performance is less than
ideal, because of reduced contrast and tube focus limitations. At the lower light
levels, performance may be poor because the population of scintillations at the
tube output includes flashes from sources other than electrons emitted by the
photocathode due to incident radiation from the scene being imaged.

The substantial achievement of theoretical performance over some part of the
operating range indicates that progress in the near future will be toward tubes
with better resolution capabilities which will approach the theoretical performance
for patterns containing finer detail and toward tubes with lower dark current to
permit long time exposure. A promising approach toward attaining these objectives,
pursued in the course of this contract, is the application of thin insulator films
as a means of pre-scanning beam image amplification.

At the start of the investigation to determine the practicability of employing
thin insulator films as image amplifiers in television camera tubes, the principle
of transmission secondary electron multiplication (TSEM) had been developed at
our Research Laboratories to the point where the feasibility of utilizing a plane-

---

parallel array of mesh supported insulating films in an image intensifier device was demonstrated[3,4]. Although a number of areas remained to be investigated, such as the fabrication of self supporting films capable of withstanding normal tube exhaust processing and the possible interaction between the photocathode and the electron bombarded films, the TSEM method of image intensification offered many potential advantages. These advantages included high resolution capability, reasonably high electron gain per intensifier stage permitting an approach to photoelectron noise limited performance, and a relatively simple method of tube construction.

The application of TSEM films as pre-scanning beam amplifiers in an image orthicon type camera tube was investigated under Contract AF33(616)-3254[5]. This work, together with related projects at our Research Laboratories[6,7], resulted in the development of reliable self-supporting TSEM films having a useful diameter of 3/4". These films were successfully used in the construction and processing of sealed-off tubes. In spite of the amplification realized in the image section, however, the low light level performance predicted for a TSEM camera tube was not achieved. This was attributed to the following possible causes which were made subjects of further study under Contract AF33(616)-8017.

(1) Spurious background arising from the combined effects of field emission resulting from high electric fields and low work function surfaces in the image section of the tube, ion currents due to residual gas in the tube envelope, photoemission arising from internal light reflections, and other mechanisms. This background emission results in a reduction of the electron image contrast ratio at the target thereby decreasing the signal to noise ratio developed by the tube, particularly at low photocathode illumination levels. By means of suitable electrode geometry, careful surface cleaning of image section components, and the use of special tube processing techniques, it has been found possible to reduce spurious emission appreciably, as experienced in our work on the intensifier-orthicon under Contract AF33(600)-39403. These experiences were applied to the work performed under this contract.

(2) Interaction between the photocathode and the TSE films and target arising from the effects of the alkali metal vapors, used in the formation of

2

the photocathode, on the surfaces of the films and target. In our inter-
action studies conducted under Contract AF33(616)-6422, photocathode
processing techniques have been developed to minimize adverse effects on
the storage target surface. An effort was made to apply these results to
the work performed under this contract.

(3)   Resolution limitations in the final TSEM dynode to target stage of the
      preamplifier section imposed by a combination of a relatively low
      accelerating voltage and the range of electron emission velocities normally
      found with a TSEM film. This was considered the principal limitation to
      image focus ability and therefore resolution. On the basis of the inter-
      action study contract, improvement in resolution capability could be
      realized by employing the thin film storage target whose secondary emission
      yield peaks at an appreciably higher primary voltage than that of the
      normal glass target, thereby minimizing the effect of TSE velocity spread.
      A more promising approach to the problem of a high resolution preamplifier,
      pursued under this contract, involved the use of a single high gain
      insulator film in the dual role of amplifier and storage target. This
      approach is fully described and evaluated in the body of the report.

In the course of the work on this contract, a low density insulator film with
demonstrated characteristics of charge image storage and fast response was developed
at our Research Laboratories. This low density KCl deposit, which exhibits high
gain and high resistivity, depends primarily on the generation of free secondary
electrons in the volume of the material, by the primary electron beam, for conduction
across the layer. The film has been employed singly either as a high gain preamplifier
stage or as a high gain target in camera tubes with both vidicon type and orthicon
type electron beam readout. It has been measured and evaluated with respect to
conventional television requirements as well as the requirements of low light level
imaging. Although no attempts have been made to measure the intrinsic resolution
capability of the film directly, the mode of operation as a high gain target
precludes the degrading effect of velocity distribution of the emitted secondary
electrons on image focus. The results show that the resolution and gain of this
type of target can exceed the performance of a phosphor-photosurface intensifier
stage. This is considered a significant comparison because intensifier-orthicon
tubes employing phosphor-photosurface intensifier stages require higher voltage

3

image sections, usually have a higher dark current background, and are difficult
to manufacture.

In the body of this report, the following section introduces the concept of
minimum detectable contrast to describe the capability of an imaging device to
discriminate between a signal and the fluctuation of the background. Section 3
presents the development, evaluation, and application of the secondary electron
conduction film as a target in camera tubes using direct beam readout. The
application of thin insulator films to image orthicon type tubes, both as pre-
amplifier dynodes and as a high gain target for low light level imaging requirements,
is described in Section 4. Included in the scope of this work was the application
of the secondary electron conduction film in camera tubes using return beam readout,
the formation of high sensitivity photocathodes, techniques to minimize adverse
materials interaction, and the reduction of spurious background.

SECTION 2
DISCUSSION OF PROBLEM

CONCEPT OF MINIMUM DETECTABLE CONTRAST

The basic problem in low light level imaging is that of being able to discriminate the signal against the fluctuations of the background ("r.m.s. noise"). In most cases background exists at the scene. Additional background of various origin and nature is introduced by the imaging device itself and can, therefore, limit the ultimate capability of such an instrument. The general problem, as well as the limitations of photoelectronic imaging devices, can be best discussed by using the concept of minimum detectable contrast, C_o.

If one defines the contrast, C, as the ratio of mean signal, S, to mean background, B, then the minimum detectable contrast becomes:

$$C_o = \frac{S_o}{B} \tag{1}$$

where S_o is the minimum signal required for a specified probability of detection. The minimum detectable signal must be k times larger than the mean fluctuation in the background, i.e.,

$$S_o = k \sqrt{B} \tag{2}$$

The factor k is called the coefficient of certainty. Its value determines the probability that a recorded signal is a true signal rather than a random fluctuation in background. For reliable detection of small image areas (in the order of a few resolution elements of the tube), k has the value of 5. For an extended area, from which the eye has much ordered information to guide it in extracting the pattern from the random noise, smaller values for k can be tolerated.

Combining Equations (1) and (2) gives:

$$C_o = \frac{k}{\sqrt{B}} \tag{3}$$

If one considers only the background arriving from the scene and neglects any

5

background generated in the detector, Equation (3) becomes:

$$C_o = \frac{k}{\sqrt{\phi A T \, \epsilon_1 \, \epsilon_2}} \qquad (4)$$

where, ϕ, is the background photon flux incident on the photocathode within the area, A, occupied by the signal, during the integration time, T. The quantum efficiency of the photocathode, ϵ_1, is expressed as the ratio of the number of photoelectrons liberated to the number of incident photons. The factor ϵ_2 is the efficiency by which the imaging device utilizes the information carried by the photoelectrons. Both ϵ_1 and ϵ_2 are bounded by zero and unity. If the gain of the instrument is high enough for the detection of single photoelectrons, ϵ_2 is usually assumed to be one. This, however, is not always justified as will be pointed out in detail later on.

Inspection of Equation (4) shows that the minimum detectable contrast for an image that occupies an area, A, on the photocathode can, for a given photon flux, be reduced by either increasing the integration time T, the quantum efficiency ϵ_1, or the utilization efficiency ϵ_2. The area, A, is fixed by the light optics used. An improvement in any one of these three quantities will, therefore, improve the overall performance of the device. Only the product of these three parameters affects the minimum detectable contrast and therefore, a decrease in one of these quantities can be compensated by increasing the product of the remaining two. Equation (4) is, of course, only valid if other sources of noise, such as amplifier noise and dark current of the photocathode and target, are not present. However, an expression identical to Equation (4) can be obtained if all the various sources of noise are combined. This results in a certain signal to noise ratio which is the same as would be obtained if the noise were due only to the genuine shot noise of the recording of photons with an "equivalent quantum efficiency" ϵ_1'[8], where ϵ_1' is correspondingly smaller than ϵ_1. Thus, the above statements are also true for the case where additional noise is introduced by the system.

PARAMETERS AFFECTING THE MINIMUM DETECTABLE CONTRAST AND THEIR LIMITATIONS

Photocathode Efficiency

Since the refinement of the multi-alkali photocathodes, it appears that little

6

is left to be gained in the photocathode efficiency, at least in the visible part of the spectrum where ϵ_1 is of the order of 0.2[9]. Since ϵ_1 can never exceed unity, improvements in only the photocathode efficiency can, at best, result in a reduction of the minimum detectable contrast, C_o, by a factor of $\sqrt{5}$.

Integration Time

There is no such theoretical limit to the benefits to be gained by increasing the integration time. Therefore, for a stationary scene, one could integrate long enough to allow detection of the desired signal. This method is utilized with photographic emulsions, for example, where one is able to record lower contrast signals than with any existing photoelectronic imaging device*. This is true despite the fact that the efficiency by which photons are utilized, corresponding to the product ϵ_1 ϵ_2 in Equation (4), is about two orders of magnitude lower than that of a good photocathode in conjunction with an amplifier that would permit registration of every single photoelectron.

There are a number of practical reasons that prevent the use of longer and longer integration times. In the case of a photographic plate, an upper limit for the integration time is set by the fact that the photographic reciprocity law is no longer valid at very low light levels where the emulsion becomes progressively less efficient. But even at higher light levels, where the reciprocity failure does not occur, the maximum integration time is limited by the finite storage capacity of the plate.

In a photoelectronic imaging device the situation is quite similar. In this case, one integrates electric charges on the surface of an insulator which forms a capacitive element together with a conductive backplate. Part of the integrated charge leaks through the insulator during the integration time. This effect is equivalent to the reciprocity failure of a photographic emulsion. When the rate of depositing charges is equal to the leakage current, it is apparent that nothing is to be gained by an increase in "exposure" time.

---

* It should be noted that the tri-alkali stabilized C.P.S. Emitron[10] is quoted as being theoretically capable of surpassing the minimum detectable contrast of a photographic plate by a factor of 10. To date, this capability has yet to be demonstrated experimentally.

The storage capacity of a photoelectric storage device is determined by the maximum amount of charge, Q_M, that can be deposited on its capacitive element. For a given capacity, C_T, and a maximum potential difference, V_M, between the plates, Q_M is given by:

$$Q_M = V_M C_T \qquad (5)$$

For the long storage times, it is therefore mandatory that the electric storage elements have as large a leakage resistance, R_T, as possible, as well as a high capacity, C_T. These requirements can be summarized as:

$$C_T R_T \gg T \qquad (6)$$

For reasons connected with the readout of the integrated information, there are restrictions on the value of C_T. This is explained in the subsequent sections, where it is shown that the leakage resistance will determine the utility of the tube for long integration times.

Photoelectron Utilization Efficiency

The third parameter that determines the performance of a photoelectronic imaging device is the efficiency by which the photoelectrons are utilized. This efficiency, ϵ_2, is defined as the ratio of the number of elements of information recorded to the total number of photoelectrons emitted. Thus, ϵ_2 is bounded by zero and unity.

The utilization efficiency is primarily determined by the gain of the tube. If each and every photoelectron experienced the same gain, G, the utilization efficiency could be expressed as the ratio of energy expended per photoelectron to the energy necessary in order to produce a scintillation. Since the available output energy per photoelectron pulse is proportional to the gain, this ratio becomes:

$$\epsilon_2 = G/G_o \text{ for } G < G_o$$

$$\epsilon_2 = 1 \text{ for } G \geq G_o \qquad (7)$$

8

where G_o is the minimum gain required for retaining the total information carried by the photoelectrons.

However, all amplification processes are subject to statistical variations and, if these fluctuations in gain are taken into consideration, the general expression for the utilization efficiency becomes:

$$\epsilon_2 = P(G \geq G_o) + \left[1 - P(G \geq G_o)\right] \ \bar{G}'/G_o \tag{8}$$

The first term in Equation (8), $P(G \geq G_o)$, is the probability that a photoelectron experiences a gain, G, greater than or equal to G_o. It is obvious that this fraction of the total number of photoelectrons will be recorded as distinct scintillations. The remaining fraction, $\left[1 - P(G \geq G_o)\right]$, will not have sufficient energy to be recorded as individual events and will convey only the portion of their initial information which corresponds to the ratio of their average gain, $\bar{G}'$, to G_o (second term in Equation (8)). This latter fraction of the total number of photo-electrons will give rise to a uniform "glow" in the image area on which the scintillations will be superimposed.

If the average gain, $\bar{G}'$, of a device is very much smaller than G_o, $P(G \geq G_o)$ approaches zero and Equation (8) reduces to Equation (7). In this case the average gain of the system determines the value of ϵ_2 and the statistical distribution is of no significance. If, on the other hand, the mean gain of the system is made very much higher than G_o, the probability that a photoelectron will experience a gain less than G_o becomes zero, and the second term in Equation (8) can be neglected, yielding an ϵ_2 of unity.

Of special interest is the case where the system gain is in the neighborhood of G_o. The utilization efficiency is now a function of the distribution as $P(G \geq G_o)$ and $\bar{G}'$ depend not only on the average gain but also on the statistical spread. Despite the fact that in this case scintillations will be visible, ϵ_2 is less than unity. (A numerical example is given in the Appendix.) It is, there-fore, not sufficient to make the average system gain equal to or slightly greater than the threshold gain for scintillations in order to achieve optimum performance, i.e., an ϵ_2 of unity. This statement is in agreement with the recent experimental results described below.

There are, to date, two types of tubes with sufficient gain to permit recording single photoelectron events, namely, the TSEM-tubes[11,12] and the cascaded image amplifiers[13] employing photocathode-phosphor combinations. It has been shown that neither the TSEM-tubes nor the cascaded type tubes are capable of recording every photoelectron[14]. This has been substantiated in measurements with the TSEM tube by one of the authors. At normal operating voltages where photoelectron scintillations can readily be seen, only about 50% of all the photoelectrons emitted result in a detectable scintillation at the output. At very much higher tube voltages, which in many cases represents the limit of safe operation, about 80% of the photoelectrons are recordable. In most applications, however, such a high tube voltage is not tolerable because the dark current due to field emission becomes very high.

For a tube whose mean gain is comparable to G_o, the effect of the statistical distribution in gain on ϵ_2 can be demonstrated by considering an example wherein the total gain is accomplished by cascading several stages. Assume that the first two stages of amplification result in a mean gain of 25. This value was chosen because it is typical for tubes employing standard TSE-multiplication where the mean gain per stage is about 5. Assume also that the rest of the system gain is such that the combined gain will permit detection of photelectrons if a photo-electron is subject to an amplification of at least 25 in the first two stages. For the first two stages, then, the threshold gain for detection of photoelectrons is 25. Figure 1 shows the calculated probability that the number of electrons, N, emitted from the second stage per photoelectron is smaller than N as a function of N. For this calculation a Poisson distribution was assumed for the number of secondary electrons emitted per primary electron*. About 50% of all the photo-electron pulses have an amplification of less than 25, the minimum value required in order to see photoelectron events. Therefore, only about half of all the photoelectrons will produce scintillations; the remainder will give rise to a general background glow. This situation can be improved by increasing the total gain of the system, thereby lowering the threshold gain for the first two stages.

---

* This assumption is believed to be valid for normal secondary electron amplifi-
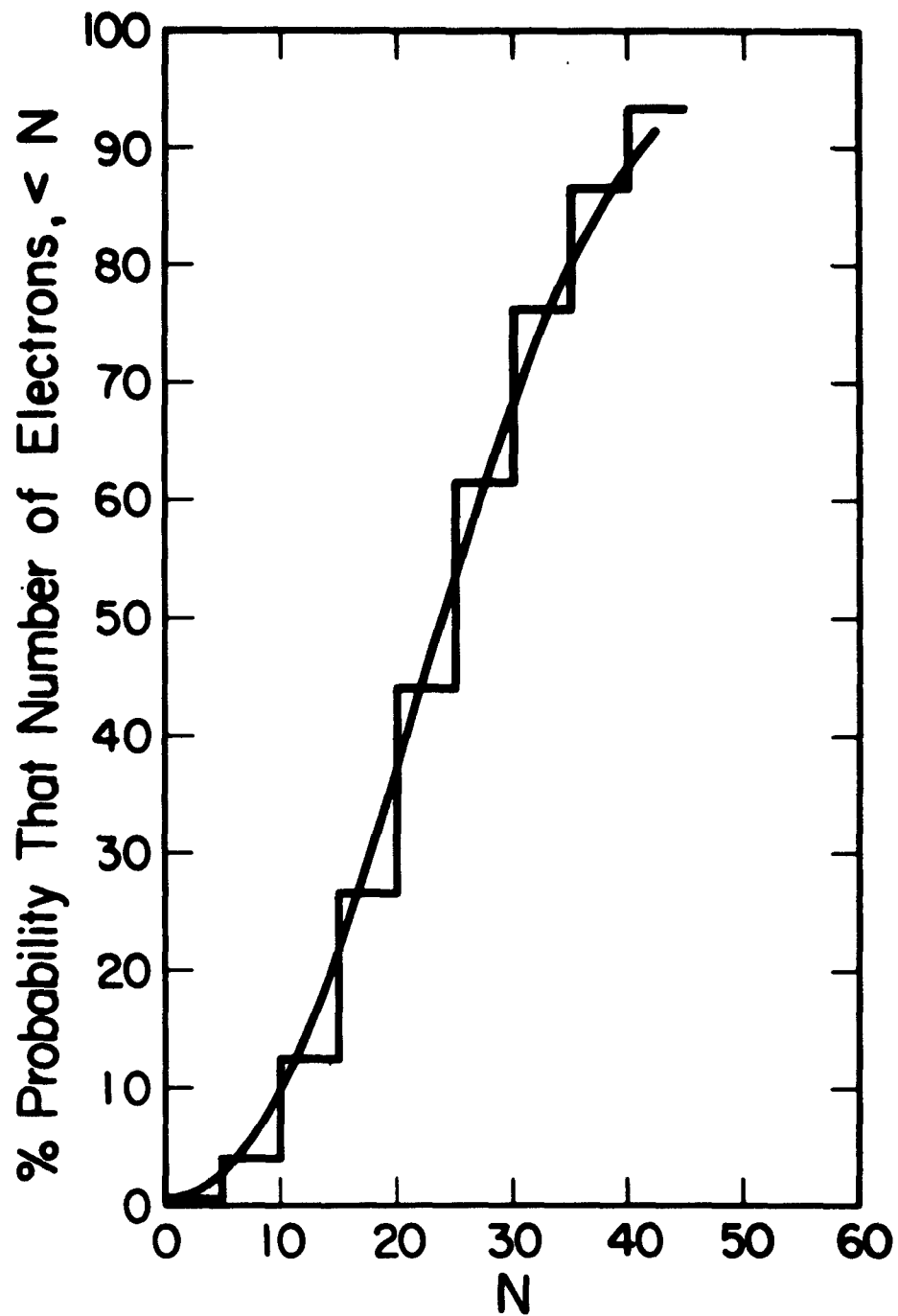 cation but may not be admissible for a different type of amplification process.

Figure 1. Emission probabilities for a combination of two dynodes, each having a mean gain of five.

From Figure 1, however, it is evident that an infinitely high gain is required in order to approach the case where all the photoelectrons will be recorded. The situation is improved considerably if the gain of the first stage is made higher. For comparison, two combinations of gain in the first stage, $\bar{G}_1$, and gain in the second stage, $\bar{G}_2$, which give the same total gain of 25 are plotted in Figure 2.

In order to reduce the statistical fluctuations in gain and, therefore, increase ϵ_2, it is important that the first stage employs a multiplication process whose relative deviation from the mean gain is as small as possible. If the amplification process obeys a Poisson distribution, it follows that the average gain of the first stage should be as high as possible, regardless of the overall gain.

SUMMARY OF BASIC REQUIREMENTS

From the preceding, one can summarize the basic requirements for a television camera tube suitable for low light level imaging and outline possible practical approaches toward constructing such a tube. While it seems impractical to try to improve on photocathode efficiency, although the photocathode with the highest quantum response in the spectral region of interest should be used, an improvement in the utilization efficiency, as well as of the integration capability appears to be feasible and will ultimately lead to the same result. The utilization efficiency for photoelectrons can be increased by:

(1) Using a return-beam multiplier in the readout section

(2) Adding one or more stages of amplification between photocathode and target

(3) Increasing the gain of the target itself

(4) Any combination of 1, 2 and 3

The integration capability can be improved by using a target with as high a resistivity as possible and a capacity as large as is compatible with lagless discharge.

The low density KCl target, which will be described in detail in the next
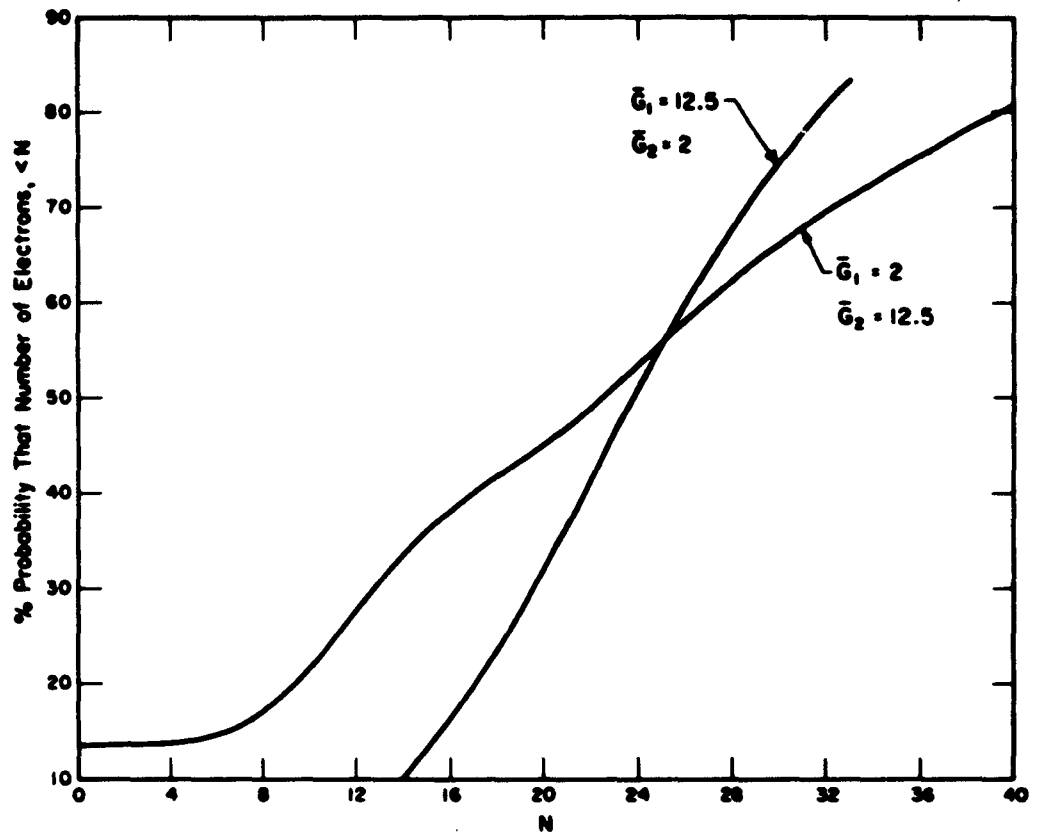
12

Figure 2. Emission probabilities for a combination of two dynodes resulting in a total mean gain of 25, where the mean gain of the first dynode is two and 12.5 respectively.

13

section, offers the advantage of high gain. Therefore, if used as the first element after the photocathode, good statistical behavior can be expected. In addition, it will be shown that the resistivity, capacity and uniformity of this target are such that long integration times are possible. Thus, several features advantageous for low light level imaging are combined in low density KCl targets.

The performance of this target, termed "Secondary Electron Conduction Target" (hereafter SEC), has been evaluated in both sealed-off tubes and in a demountable vacuum system. The details of these tubes are described in the following sections.

SECTION 3
EXPERIMENTAL TUBES USING DIRECT BEAM READOUT

DESCRIPTION OF TARGET

The target consists of an aluminum oxide film, of about 1000 $\overset{o}{A}$ thickness, supported on a 5/8 inch diameter metal ring. A layer of 500 $\overset{o}{A}$ of aluminum, deposited on the aluminum oxide by vacuum evaporation, serves as the conducting electrode. The aluminum is covered by a layer of KCl "smoke",[15] which is formed by evaporating the KCl in an inert gas atmosphere at a pressure of a few millimeters of mercury. The density of such a layer is only about two percent of the bulk density of KCl. A typical thickness is 25 microns which corresponds to a mass per unit area of 100 $\mu gm \ cm^{-2}$. (bulk KCl density = 1.984 $gm \ cm^{-3}$)

OPERATION OF TARGET

The details of operation are explained schematically in Figure 3. Electrons with an energy of approximately 10 KeV impinge onto the target from the aluminum oxide side. This energy is high enough for them to penetrate the aluminum oxide layer and the aluminum electrode and to dissipate most of their energy within the low density layer of KCl, thereby creating low energy secondary electrons. If, prior to the impact of a primary electron, the target has been polarized by applying a positive voltage to the backplate and stabilizing the exit surface at ground potential (gun cathode potential), these low energy electrons will cause the exit surface to change its potential to more positive values due to conduction across the layer and secondary electron emission from the exit surface. The scanning beam is used to replenish this charge, resulting in a current pulse through the video resistor. While at first the conduction through the layer dominates and secondary electron emission contributes only a small fraction of the total change in charge, a typical ratio is 25:1, the situation reverses whenever the exit surface potential approaches backplate potential. The conductivity becomes zero while secondary emission continues and drives the exit surface potential beyond target backplate potential, causing the electric field across the layer to reverse polarity. When the exit surface becomes a few volts positive with respect to the backplate, conduction again takes place, however, in the reverse direction. The exit surface potential will stabilize at an equilibrium potential determined by the voltage at which the number of secondary electrons leaving the surface equals the number of
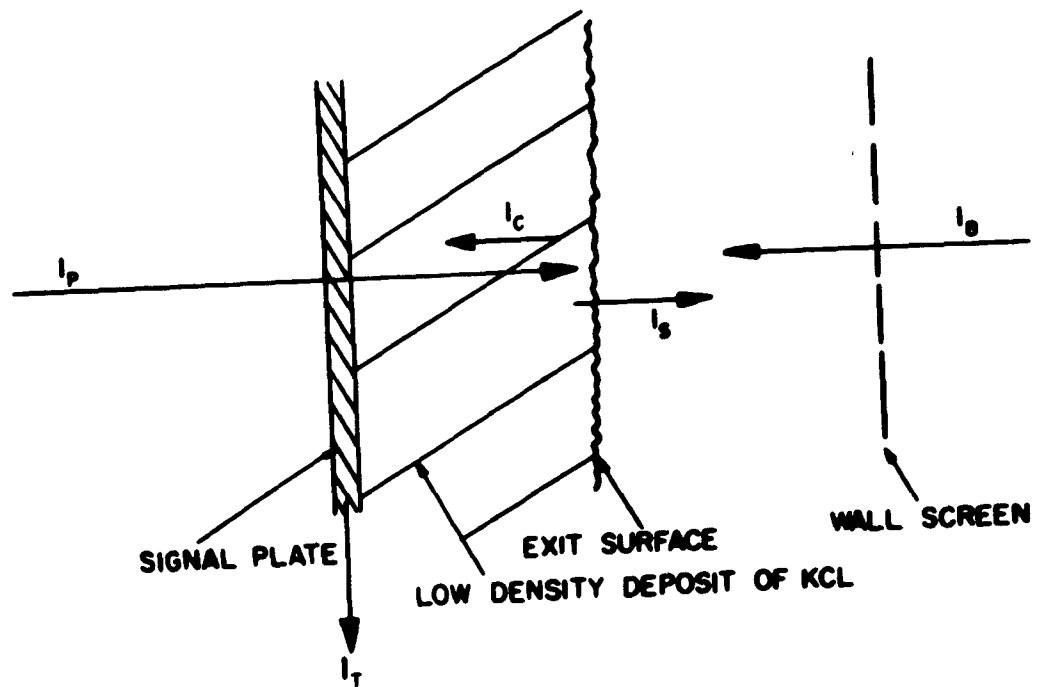
15

Figure 3. Schematic of target operation

conducted electrons. The equilibrium potential is generally higher than the first crossover potential for secondary electron emission in reflection. This means that if the target has been charged beyond crossover potential, due to high input current densities or long integration times, the reading beam will not return the surface to gun cathode potential but will stabilize the exit surface at wall screen potential. The result is that the video current changes its direction and a negative picture is displayed on the monitor. This effect is similar to the target behavior of the CPS Emitron[10]. The target can be returned to its normal mode of operation by temporarily lowering the wall screen potential below the first crossover potential. The tendency for the exit surface potential to "run away" may be prevented if an additional grid is inserted at a suitable distance between the exit surface and the wall screen and is maintained at a potential below that of first crossover.

DESCRIPTION OF TUBES

The performance of the SEC targets was tested in tubes consisting basically of a photocathode, the target and a conventional vidicon gun. A schematic cross section of these tubes is shown in Figure 4. This tube, except for the target, is known as the Uvicon, an ultraviolet sensitive tube being developed by Westinghouse for the Smithsonian Astrophysical Observatory, Cambridge, Massachusetts[16]. The photocathode has a diameter of 1.2 inches and consists of CsI with palladium as a conductive substrate deposited on a lithium fluoride window. The photoelectrons are accelerated by approximately 10 KV on to the 5/8 inch diameter target. Focusing of the image section is accomplished by an electrostatic lens system.

In addition to these tubes, a magnetically focused demountable system was used for target studies. This system, shown schematically in Figure 5, was primarily constructed for preliminary target evaluation, including a study of resolution limitations of the target. The results obtained with both types of tubes are described below.

MEASUREMENTS

Gain

Under the impact of a primary electron, a large number of free electrons are created within the layer. A fraction of these electrons escape from the exit surface
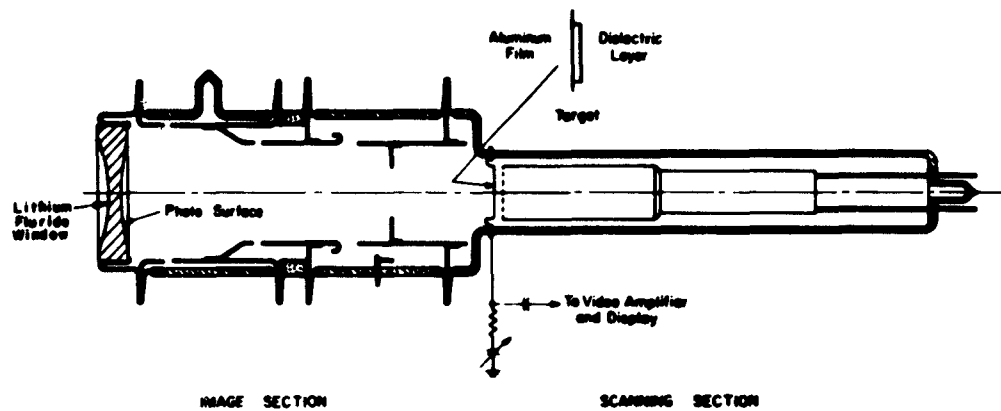
16

Figure 4. Cross section of sealed-off tubes used for target
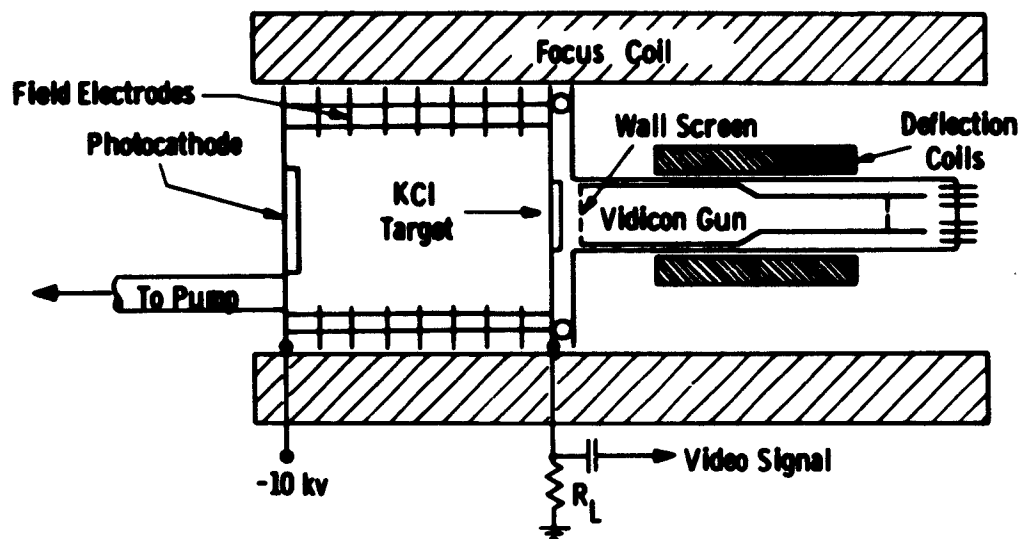performance evaluation

Figure 5. Cross section of demountable system with magnetic focusing

of the target and are collected by the wall screen. These transmitted secondary electrons represent the current, I_s, in Figure 6. The rest of the electrons liberated within the target are normally not observed since they are absorbed after a number of collisions within the target material. However, if an electric field is applied across the target, these electrons can be transported through the layer. They give rise to a conduction current, I_c.

It should be kept in mind, however, that these are free electrons traveling in the interparticle volume of the layer, contrary to electrons in the conduction band. This statement is based on response time measurements which show that the response of such a layer is very much faster than that for solid state conduction[16] In addition to free electrons created within the layer, electrons are probably also excited into the conduction band. However, their contribution to conduction across the layer is insignificant at normal target voltages (corresponding to a field of only about 1 KV/cm) due to the interparticle barriers.

If the polarity of the electric field applied across the layer is such that the free conduction electrons are collected on the signal plate, the secondary current I_s, as well as the conduction current, I_c, will charge the exit surface positive. The scanning beam, I_B, then replaces this charge and a signal current, I_T, is generated in the target lead.

Assuming uniform illumination, the total charge stored, Q_s, on one resolution element of an area, a, during one frame time τ, is:

$$Q_s = \frac{I_c + I_s}{A} \cdot a \cdot \tau \qquad (9)$$

where A is the scanned area, and I_c and I_s are the total conduction current and secondary current respectively. This charge is then replenished by the beam within the dwell time $\Delta\tau$, resulting in a signal current I_T. Thus,

$$I_T = \frac{Q_s}{\Delta\tau} = \frac{I_c + I_s}{A} \frac{a\tau}{\Delta\tau} \qquad (10)$$

Since

$$a\tau = A\Delta\tau \qquad (11)$$

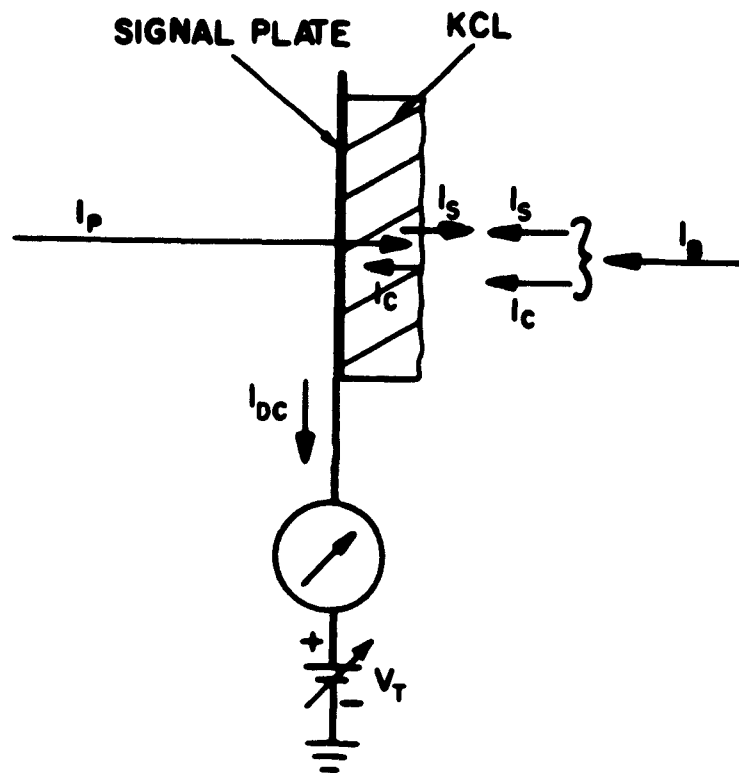we find

$$I_T = I_c + I_s \qquad \cdots \qquad (12)$$

19

Figure 6. Schematic diagram of currents involved in
target operation

If one now defines as "AC-gain", G_{AC}, the ratio of signal current to primary current, Equation (12) leads to

$$G_{AC} = \Delta + \delta \qquad\qquad (13)$$

where,

$$\Delta = \frac{I_c}{I_p} = \text{conduction gain}$$

and,

$$\delta = \frac{I_s}{I_p} = \text{secondary gain}$$

In this type of target, then, the secondary gain, as well as the conduction gain, are utilized to amplify the primary current, I_p.

With increasing voltage on the signal plate, conduction current due to electrons that have been raised into the conduction band will take place and the observed gain will increase by this third component. If the contribution of conduction band electrons to the gain is appreciable, the target shows the typical time lag characteristic for electron bombardment induced conductivity (EBIC). This effect is not present at low target voltages. Solid state conduction seems to take place only after a certain threshold voltage is exceeded on the target. This threshold voltage lies between 5 and 25 volts, depending on target thickness and structure.

Typical gains in the fast mode (erase time in the order of one frame time) are 200. Gains that include solid state conduction can be as high as one thousand.

In order to measure the gain, the target was connected to a vacuum tube electrometer in series with a battery (which supplied the target voltage) to ground. For a constant photocurrent and continuous scanning, the direct current, as indicated by the meter, is the conduction current plus the primary current:

$$I_{DC} = I_c + I_p \qquad\qquad (14)$$

If one defines as "DC-gain", G_{DC}, the ratio of this DC-current to the primary

21

current:

$$G_{DC} = \Delta + 1 \qquad (15)$$

It follows from Equations (13) and (15) that

$$G_{AC} = G_{DC} + \delta - 1 \qquad (16)$$

Since the DC-gain can be measured in the way described above and since the secondary gain, δ, is easily determined by measuring the secondary current collected by the wall screen while the scanning beam is off, G_{AC} can be calculated according to Equation (16). A typical measurement of this type is shown in Figure 7 where the conduction gain is plotted as a function of applied target voltage. The gain due to transmitted secondary electrons (TSE) is also plotted in the same diagram. During this measurement, the wall screen was at a potential of 100 volts positive with respect to the target backplate. Therefore, the TSE gain was highest when the target backplate potential was zero. It approaches the intrinsic yield of KCl (7 to 8) when the potential difference between wall screen and target backplate is zero, which, in this particular case, occurs at 100 volts on the target backplate. It is seen that the total gain, essentially the sum of conduction gain and TSE gain, reaches a value of 300 at 25 volts target voltage.

It is also evident that at zero target voltage the target gain is still appreciable, approximately 60, contrary to the normal EBIC-target where no gain is measured at this point. Even at negative target voltages, the target will continue to exhibit gain because secondary emission continues. In this case the conduction current flows in the opposite direction and therefore substracts from the TSE gain. At the point where the contribution to gain due to TSE is equal and opposite to that due to conduction, no gain will be observed.

The contribution of transmitted secondary electrons and conduction electrons to the total gain as a function of the exit surface potential of the target is schematically shown in Figure 8a. The potential V_T denotes the target backplate potential. Figure 8b shows the integrated signal as a function of the exit surface potential.

22

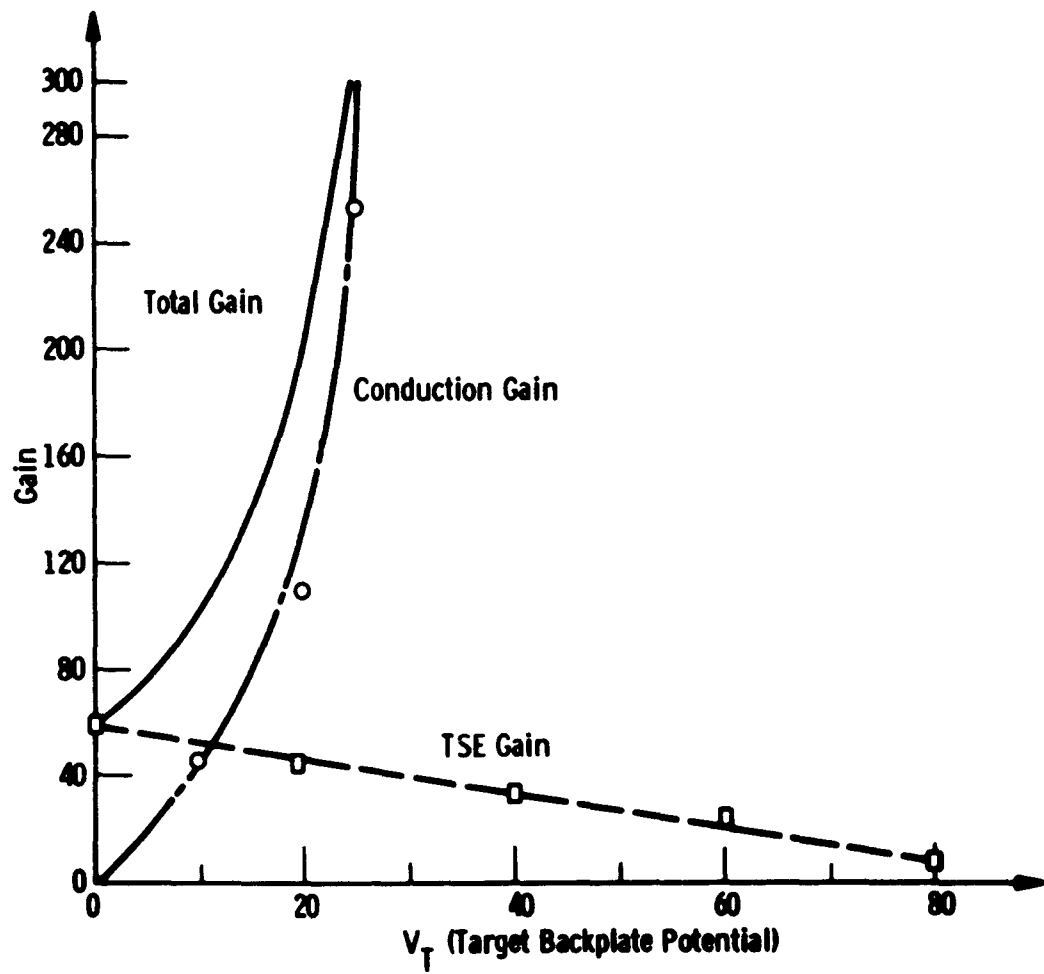Figure 7. Contribution of conduction gain and secondary gain to total gain as a function of target backplate potential.

23

Figure 8a. Conduction gain, secondary electron gain and total gain as a function of target surface potential, V_s (schematic)
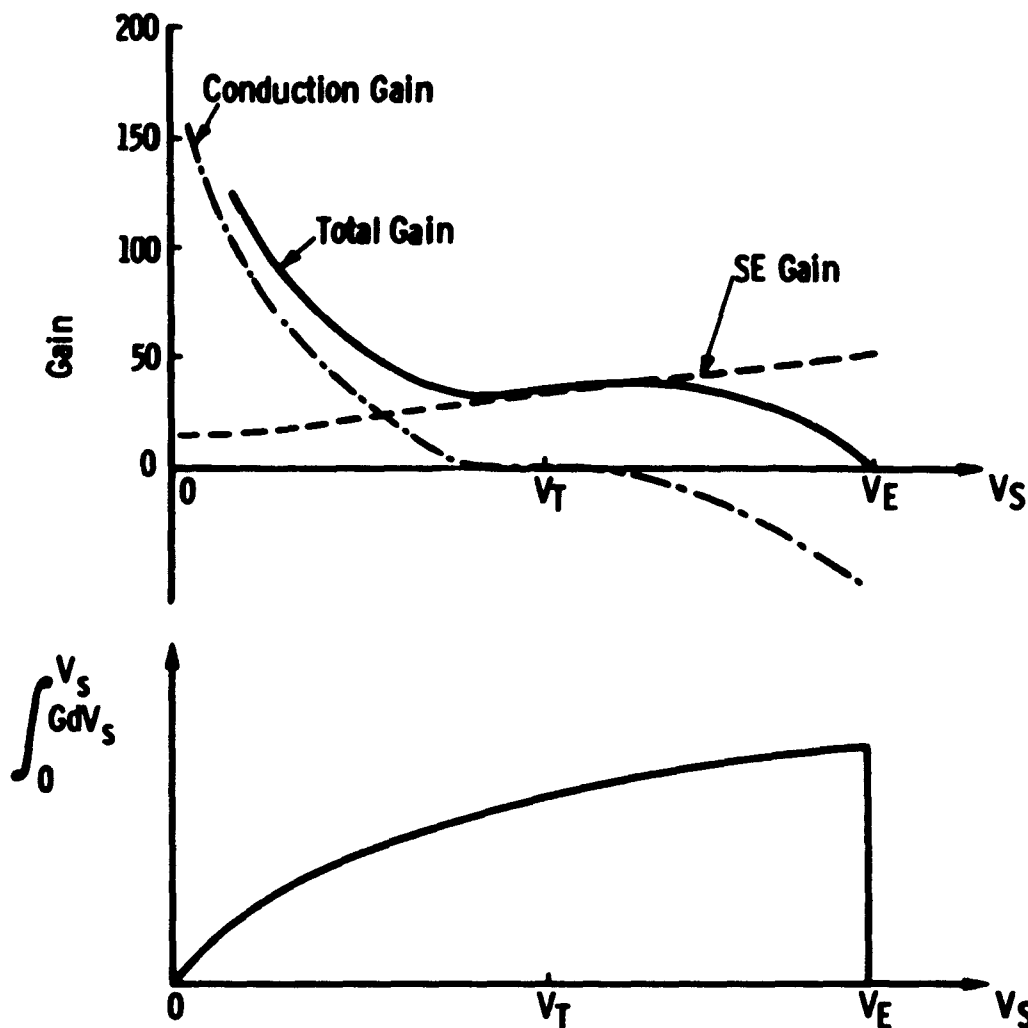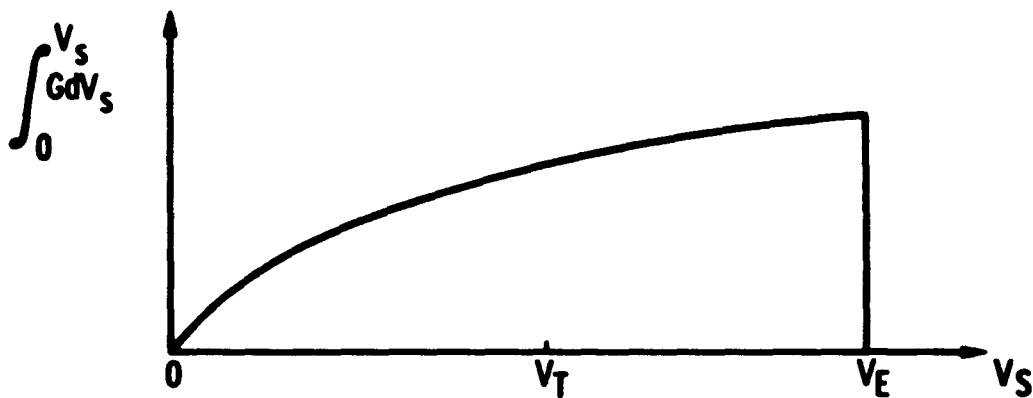

Figure 8b. Accumulated "signal" as a function of target surface potential, V_s (schematic). V_T denotes target backplate potential, V_E denotes equilibrium potential.

24

Response Time

For almost all applications of camera tubes, it is essential that the information stored on the target, in the form of electrical charges, can be read out by the scanning beam within one frame time, 1/30 sec. at standard scanning rates. (When the signal is displayed on a monitor and observed by the eye, this requirement is eased to the storage time of the human eye, which is 0.2 sec.)

Several reasons for the above requirement exist. Some of these result from practical considerations connected with a specific application, such as the undesired "stickiness" of pictures of moving objects. Some are of fundamental importance. For example, the signal current resulting from a certain charge, Q, being read off by the scanning beam within the time T is inversely proportional to the time T. Thus, under otherwise equal conditions, a system with a longer readout time constant will have a poorer signal to noise ratio. The mere quotation of a target gain computed from dc currents does not, therefore, allow any quantitative conclusions about the performance of a camera tube whose target exhibits a long readout time constant. It seems more reasonable to use the product of steady state gain, G^*, and $\frac{\tau}{T}$ instead, where T is the time for a signal to decay to some specified value of its initial amplitude and τ is the frame time:

$$G = G^* \frac{\tau}{T} \; ; \; \text{with} \; T \geq \tau \qquad (17)$$

There are two sources of time lag in the type of camera tube described above. The first is the inability of the beam to discharge the target within one frame time, and the second is the finite decay of the conduction process in the target after the excitation by primary electrons has been terminated.

The time constant for the discharge lag is given by the product of target capacity, C_T, and "beam resistance", R_B. The beam resistance in turn is a function of the velocity distribution of the beam electrons and the potential difference between gun cathode and the target area scanned. Typical values of R_B, for standard vidicon guns, are 10^6 ohms at 2 volts and 10^7 ohms at 0.5 volts[17]. The beam resistance approaches infinity as the target potential approaches gun cathode potential.

Since the beam resistance is fixed* at about 10^7 ohms for small voltage excursions, the target capacity has to be less than 1/30 sec. divided by 10^7 ohms,

$$C_T \leq 3 \times 10^{-9} \text{ farads} \tag{18}$$

in order to achieve lagless discharge. The SEC target is about 25 μ thick and the dielectric constant, ϵ , is very close to unity since about 98% of the volume is vacuum. Therefore, the calculated target capacity will be only 67×10^{-12} farads for an area of 1.9 cm^2, and no discharge lag should occur.

The time lag due to the slow decay of conduction in the layer after excitation is a more serious problem. Generally, it is found that photoconductive targets (or EBIC targets) that exhibit a high gain also show an excessive time lag. If one would use, however, free electrons for the signal generating mechanism, as is done in the SEC target, this time lag should not be observed.

Measurements to determine the time lag were made in the following manner. The video signal was displayed on the Y-axis of an A-scope. Since interlaced scanning and a time sweep of 0.1 sec./cm was used, six "field pulses" per centimeter were displayed on the X-axis. The illumination on the tube, resulting in a photocathode current of 10^{-11} amps, was turned on for about 0.4 sec. using a mechanical shutter. Figure 9 is a photograph of the oscilloscope trace showing that the rise time as well as the decay time of the video signal is shorter than 1/30 sec., which is the shortest time that can be measured with this technique. For comparison, the residual signals for a Vidicon in the low and high velocity scanning modes are plotted, in Figure 10, as a function of the number of scans. These data are taken from Reference(18).

The fact that no time lag can be observed at normal operating voltages substantiates the evidence that the signal generating mechanism is due to, or largely due to , free electrons created by the primary electrons and collected

---

* Attempts have also been made to reduce R_B by using "monochromatic" guns or high velocity scanning(18).
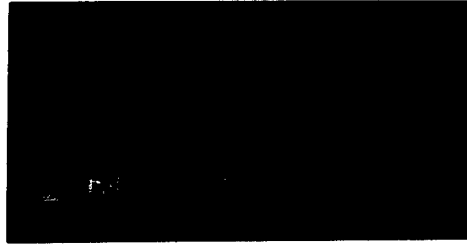
26

Fig. 9 - Video signal (Y-axis) as function of time. Time scale (X-axis): 0.1 sec/cm.
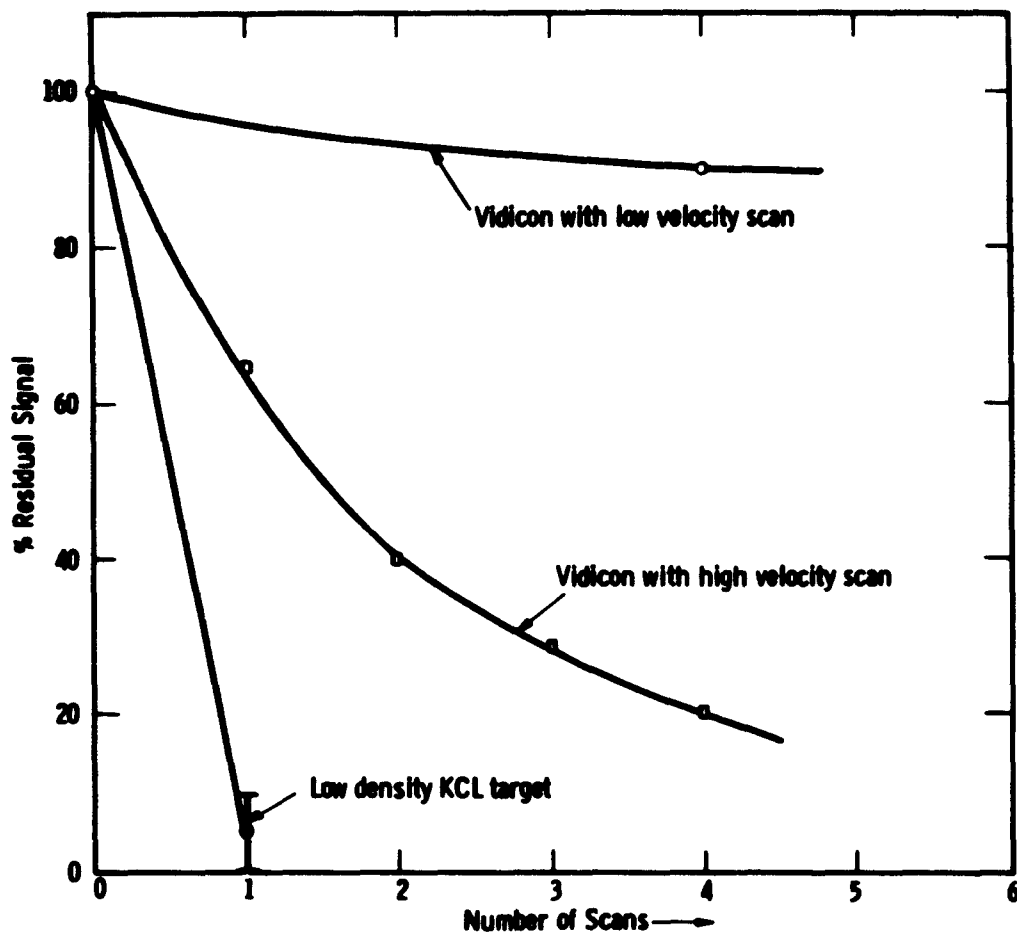
Figure 10. Residual signal as a function of number of scans for a Vidicon and for a tube with a low density KCl target

either by the backplate or by the wall screen. If the target voltage is increased beyond these voltages, a time lag becomes noticeable. This can be explained by the fact that the electric field within the layer is now high enough to permit significant solid state conduction. The onset of the conductive lag is associated with an increase in gain. One, therefore, has the choice of operating the target at relatively low voltages in the fast mode with a gain of about 200, or operating at higher voltages and thereby sacrificing speed of response in favor of higher gains.

Integration

The two most important parameters effecting the integration characteristics of a tube are the target capacity, C_T, and the target resistance, R_T. In order to be able to integrate for a certain time, T_I, the following condition has to be met:

$$R_T \ C_T > T_I \tag{19}$$

with

$$R_T = \rho \ \frac{d}{A} \tag{20}$$

and

$$C_T = \epsilon \ . \ \epsilon_o \frac{A}{d} \tag{21}$$

where d, is the target thickness, A, the target area, ρ , the resistivity, $\epsilon_o = 8.9 \times 10^{-14}$ amp sec./volt cm, the vacuum dielectric constant and ϵ , the dielectric constant of the target. Substituting for R_T and C_T, Equation (19) becomes:

$$\rho \epsilon \ \epsilon_o > T_I \tag{22}$$

It is, therefore, important to make the resistivity as high as possible in order to achieve long integration times. As an example, consider the case where one wishes to integrate a weak signal for one hour with the SEC target ($\epsilon = 1$). One finds from Equation (22) that the resistivity, ρ , must be greater than 4×10^{16} ohm cm.

There are, however, two additional requirements that have to be fulfilled for long-time integration. The first one is that the tube dark current (thermionic emission from the photocathode and field emission) must be small compared to the signal current. The second one is that the integrated signal must be small enough to keep the target from saturating, i.e.,

$$j_{PC} \leq \frac{C'_T \, V_M}{\bar{G} \, T_I} \qquad (23)$$

where, j_{PC}, is the photocurrent density, $\bar{G}$, is the average target gain during the integration time, T_I, and V_M is the maximum permissible voltage excursion of the target exit surface. C'_T is the target capacity per unit area. Measurements described in a later section have shown that the SEC target is capable of storing a charge of 3×10^{10} electrons per cm^2 before saturation is reached. For an average target gain of 200, this means that approximately 10^8 photoelectrons per cm^2 are needed to exhaust the storage capacity of the SEC target*. If, for example, a signal is integrated for one hour, it follows that the photocathode current density should be less than 1×10^{-14} amps/cm^2. If, however, the target is operated at a lower gain (achieved by reducing the primary voltage), the number of photo-electrons that can be stored will increase accordingly. This latter method should be used if one wants to discern low contrast objects which occupy only small areas on the photocathode of the tube, and, therefore, require a large number of photo-electrons for recognition.

In order to measure the resistivity of the target and to check its integration capability, the following experiment was conducted. A tube with a UV-sensitive photocathode (CsI), used because it exhibits low thermionic emission, was illuminated on only half of its photocathode area, the other half was masked. The photocurrent density was 10^{-16} amps/cm^2. This current was determined by first measuring the photocathode current as a function of the distance, R, between the photocathode and the light source over a range of 10^{-8} amps to 10^{-12} amps, and

---

* An Eastman Kodak 103a-0 plate is quoted as having a storage capacity of 10^7 events per cm^2 [19].

30

then extrapolating the current versus $1/R^2$ plot to 10^{-16} amps. The video signal was connected to the vertical deflection plates of an A-scope properly triggered to present one selected scanning line. The time sweep was one μsec./cm. The scanning beam was turned off and the signal was integrated on the target for various lengths of time, after which the beam was pulsed on and the integrated signal was photographed from the A-scope. Figure 11 shows three such photographs after integration times of 3 minutes, 8 minutes and 15 minutes. (For the exposure showing 15 minutes integration, the vertical deflection sensitivity of the A-scope was reduced by a factor of five.) Still smaller signals have been successfully integrated for 1.5 hours. These experiments demonstrate that it is possible to integrate extremely weak signals for periods up to hours without background contribution due to target leakage current. Therefore, the target leakage current, I_L, is considerably less than the integrated signal current, times the target gain, i.e.,

$$I_L \ll 2 \times 10^{-14} \text{ amps}$$

With a target voltage of 10 volts, the resistivity is therefore found to be greater than 10^{17} ohm cm.

Regeneration

Regeneration is the term used to describe the reappearance of a signal after initial erasure by the scanning beam. If a signal is impressed on an ordinary photoconductive (or EBIC) target, some of the carriers thereby generated may be trapped[20]. These trapped carriers do not immediately contribute to the signal during readout, but are released slowly and thereby retain a fraction of the signal for later readout. If the target is not scanned continuously, as is the case during prolonged integration, a signal corresponding to the original image is regenerated by simultaneous integration of carriers released from the traps and carriers generated by the present exposure. It is evident that this effect is undesirable and must be avoided since it is an additional source of background.

In order to measure the regeneration property of the SEC target, the tube was exposed to a relatively strong signal (10^{-10} amps/cm^2 photocathode current density). The illumination was then turned off and immediately thereafter the
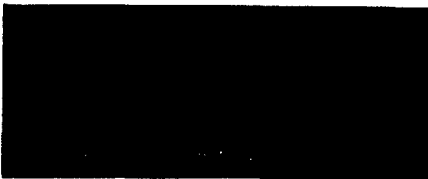
Fig. 11 - Integrated signal (single line) after 3 min, 8 min and 15 min.

scanning beam was interrupted. The scanning beam was pulsed on again after a suitable time interval, and the monitor was observed for a regenerated image. No trace of a regenerated image could be seen even after time intervals as long as 15 minutes. It is therefore concluded that trapped carriers, which invariably occur, cannot generate an image in the SEC target. This is taken as further evidence that solid state conduction through the target is excluded at normal target voltages, possibly due to the many interparticle barriers that exist across the target thickness. Therefore, only free electrons traveling in the interparticle volume are believed to provide the necessary charging current for signal generation. This conclusion is further substantiated by the fact that no time lag was observed.

Resolution

One must distinguish between the resolution capabilities of the target, the maximum resolution of a tube incorporating such a target and the resolution limitations set by the associated equipment. No attempts have been made to measure the intrinsic resolution capabilities of the SEC target directly. Based on the thickness of the target (25μ), it seems reasonable, however, to assume that up to 75 TV-lines/mm should be resolvable on the target before scattering of the primary electrons significantly degrades the resolution.

Resolution measurements have been made with sealed-off Uvicon tubes using electrostatic focusing in the image section and with demountable tubes employing all magnetic focusing. In the first case, the maximum resolution was found to be 300 TV-lines/inch as referred to the photocathode, or 600 TV-lines/inch on the target, as these tubes employ a linear minification of 2:1 in the image section. Figure 12 is a photograph of a 100% contrast test pattern as reproduced by one of these tubes. The tubes with magnetic focusing of the image section clearly resolved 1000 TV-lines/inch on the photocathode, indicating that in the electrostatically focused tubes the upper limit to resolution is set by the electron optics. The resolution obtained with the magnetically focused system was limited by·the bandwidth of the video amplifier.

The above results show that tubes with SEC targets can be operated to give standard television resolution (525 lines). With a more refined system, for example, magnetic focusing of the image section combined with slow scan readout,
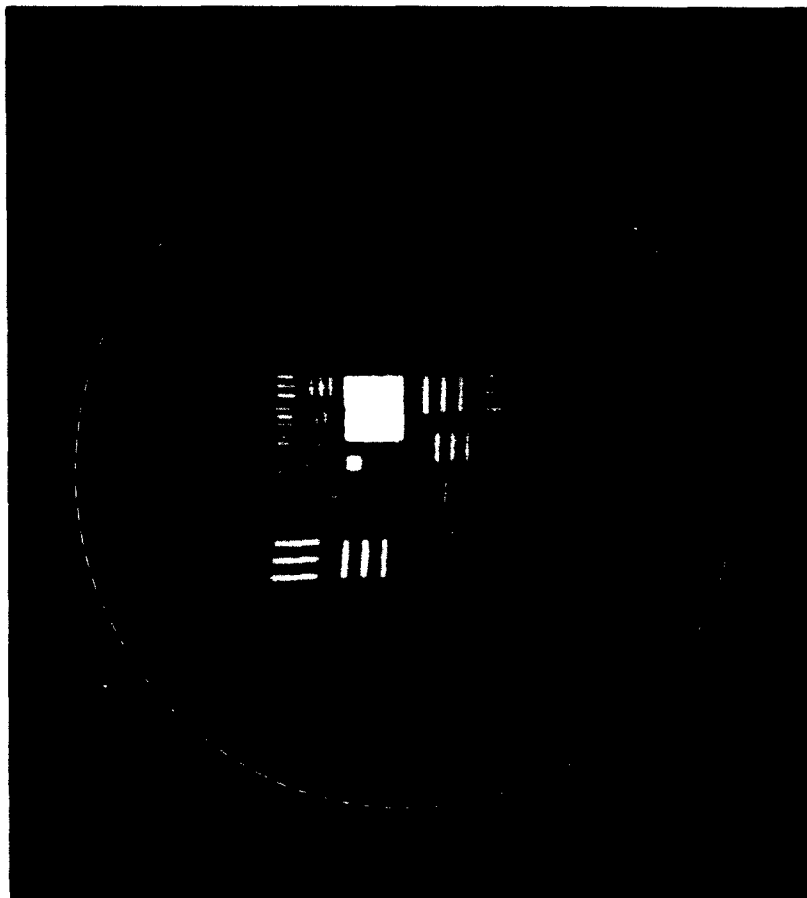
33

Fig. 12 - Resolution pattern as transmitted by electrostatically focused tube;
dotted line indicates target diameter.

it is believed possible to obtain even higher resolution.

Minimum Detectable Signal

In estimating the minimum detectable signal, expressed in terms of number of photoelectrons per frame time, τ , and resolution element, a, the criterion discussed previously on the concept of minimum detectable contrast is used. For reliable detection, the signal has to exceed the noise (fluctuation in background) by the certainty coefficient, i.e.,

$$S \geq k\ N \tag{24}$$

If it is assumed that a 100% contrast signal (no scene background) and no dark current and target leakage current exist in the tube, then the only source of noise is that of the preamplifier used to transmit the video signal. The preamplifier noise, arising from the thermal noise of the load resistor and the shot noise of the plate current of the first amplifier tube, is customarily described by a "noise equivalent current", I_N, flowing through the load resistor. Thus, Equation (24) becomes:

$$Q_s \geq k\ I_N \Delta\tau \tag{25}$$

where Q_s is the charge deposited by the signal on the target during one frame time, τ , and $\Delta\tau$ is the dwell time of the readout beam on the signal area.

Since Q_s is equal to the number of photoelectrons, n, emitted per frame time and resolution element, times the target gain, G, times the electron charge, e_o, we have:

$$Q_s = n\ G\ e_o \tag{26}$$

Combining Equations (25) and (26) gives:

$$n \geq \frac{k\ I_N\ \Delta\tau}{e_o\ G} \tag{27}$$

Substituting $\frac{a}{A} \cdot \tau$ for $\Delta\tau$ (Equation (11)) and using the fact that

$$A = N^2 a \tag{28}$$

where, N, is the number of resolvable TV-lines, Equation (27), the expression for the minimum number of photoelectrons per resolution element and frame time, needed for detection, with a certainty coefficient of 5, becomes:

$$n \geq \frac{5 \, I_N \, \tau}{e_o \, G \, N^2} \tag{29}$$

A practical value for I_N that can be achieved with a preamplifier of 8 Mcs bandwidth is 2×10^{-9} amps. The normal frame time, τ, is 1/30 sec. Assuming a useful target gain of 200 and 525 line resolution, the minimum number of photoelectrons needed per frame time and resolution element to give reliable detection is, according to Equation (29), 40.

From experiments carried out with sealed-off tubes employing photosurfaces, the minimum detectable signal was found to correspond to less than 100 electrons per resolution element and 1/30 sec. frame time, in good agreement with the above estimate.

Dynamic Range

The dynamic range of a target is defined as the ratio of the maximum signal that the target can store without saturating to the minimum detectable signal. Its value is a measure of the ability of the target to successfully portray scenes containing highlights as well as shadows. A faithful reproduction of such a scene is dependent upon the complete transfer characteristic of the target which, for the SEC target, has been presented qualitatively in Figure 8b.

The maximum charge the target can store is given by Equation (5). Multiplying Equation (25) by the number of resolution elements, N^2, and substituting τ for $\Delta \tau \, N^2$, gives the minimum charge that can be detected with a system using direct beam readout. Thus, the dynamic range, D, is given by:

$$D = \frac{V_M \, C_T}{k \, I_n \, \tau} \tag{30}$$

For the SEC target, V_M is simply given by the first crossover potential of the low

density KCl layer. A practical value for V_M is 20 volts. Using $C_T = 67 \mu\mu f$, a frame time of 1/30 sec., an equivalent noise current of 2×10^{-9} amps and a coefficient of certainty of 5, Equation (30) gives a dynamic range of approximately 4.

The dynamic range of the SEC target was measured under the above conditions and was found to be 50, or about 12 times the calculated value. Since the maximum voltage excursion, V_M, was not measured simultaneously and since crossover potentials of as high as 80 volts have been observed for these targets, it is possible that the voltage excursion permitted during this measurement exceeded that used in the calculation by a factor of as much as 4. The remaining factor, of at least 3, between the calculated and measured values of the dynamic range can be attributed to the simplification used in calculating the target capacity. This calculation was based on the assumption that all the stored charge is located at the exit surface. In reality much of this charge is within the KCl layer and, therefore, the "capacitive thickness" is smaller than the physical thickness*. Thus, it appears that the true value for C_T is approximately 200-800 $\mu\mu f$.

Although the capacitance of the SEC target is less than that of Vidicon targets, the permissible voltage excursion of the SEC target is greater. Since the competing noise is the same for all targets using direct beam readout, the dynamic range of the SEC target is comparable to that of the Vidicon. Compared to the image orthicon, both the capacitance and permissible voltage excursion are greater for the SEC target. Thus, if return beam readout is employed in combination with the SEC target, a dynamic range greater than that of the image orthicon is expected.

Target Uniformity

While the integration capability of a thin film of photoconductive (or EBIC) material is primarily determined by the absolute amount of leakage current due to

---

* Charge storage within the layer is compatible with fast readout in this case since the electron beam is able to penetrate into the spongy layer.

polarization, local variations in leakage current will generate additional background and further limit the integration capability. In its most pronounced form, this latter effect will show up as so called "bright spots". It is evident that the presence of such background signals is not desirable in most applications using short integration times (standard frame rates). It cannot be tolerated at all for long-time integration of low contrast signals. In the construction of camera tubes using standard EBIC targets, this problem necessitates pretesting and selecting the targets. In practice, however, one has to compromise very often between gain and uniformity. All of the SEC targets investigated so far (approximately 30) have shown extremely good uniformity. None of the tubes built with these targets showed "bright spots" at normal operating voltages despite the fact that the targets were not preselected. This is not too surprising because the field across the target material is only of the order of a few KV per centimeter, contrary to the standard EBIC target which operates at comparable gains only if the electric field is at least one order of magnitude higher. Even after long integration times, no background due to nonuniform discharge has been noticed. This has been demonstrated in the section on integration.

Life Time

An important parameter regarding the practical application of a target in camera tubes is its life time. Measurements of the life time of the SEC target have been made in the following manner: A target which had been sealed into a dummy tube together with a photocathode and a collector electrode was operated for a period of 10^3 hours. The photocathode current was 4×10^{-9} amps and the secondary current approximately 2×10^{-7} amps, which corresponds to a secondary gain of 50. The total charge passed through the target was 0.8 coulombs. After the life test was completed, no measurable decrease in secondary gain was detected. Since typical photocathode currents encountered in the actual application of tubes using this target are expected to be less than 10^{-9} amps (10^{-9} amps/cm^2 photocurrent density corresponds to an illumination of 10^{-2} ft-candles, assuming a 100 μA/lumen photocathode efficiency), it is felt that the life time of such a tube will be limited by other parameters rather than by the target.

SECTION 4
EXPERIMENTAL TUBES USING RETURN BEAM READOUT

TSE INTENSIFIER-ORTHICON

As described earlier, the application of transmission secondary emission films as pre-scanning beam amplifiers was initiated under Contract AF33(616)-3254[5]. In the course of this investigation, the feasibility of using TSEM films as prebeam amplifiers in camera tubes with return beam readout was demonstrated. Operable tubes with two stages of self-supporting TSEM dynodes were constructed and evaluated. These tubes exhibited limiting resolution in the order of 400 - 500 TV lines. The range of photocathode illumination over which the tubes operated was in the order of 10^{-5} to 10^{-2} ft-candles. Measurements taken in the image section of sealed-off tubes showed that gains of 25 or higher were attained with two TSEM dynode stages. In spite of the prebeam amplification realized, however, the expected performance at low light levels was not observed. The possible causes can be summarized as follows:

(1) Spurious background which degrades the signal to noise ratio at the target.

(2) Interaction between the photocathode and the TSEM films and target.

(3) Combined effect of a relatively low accelerating voltage and the range of transmission secondary electron emission velocities on image focus, in the final TSEM dynode to target stage.

(4) Abnormally low secondary emission yield of the return beam multiplier section.

These possible causes limiting predicted tube performance were investigated under the present contract. In this study, the successful experiences in our work on the intensifier-orthicon and the thin film storage target orthicon, relative to these problems, were applied.

A magnetically focused TSE image intensifier was designed for high voltage operation with radially supported electrodes, as shown in Figure 13. The purpose

39

TSE IMAGE INTENSIFIER

Photocathode

Radial Support

TSEM Dynode

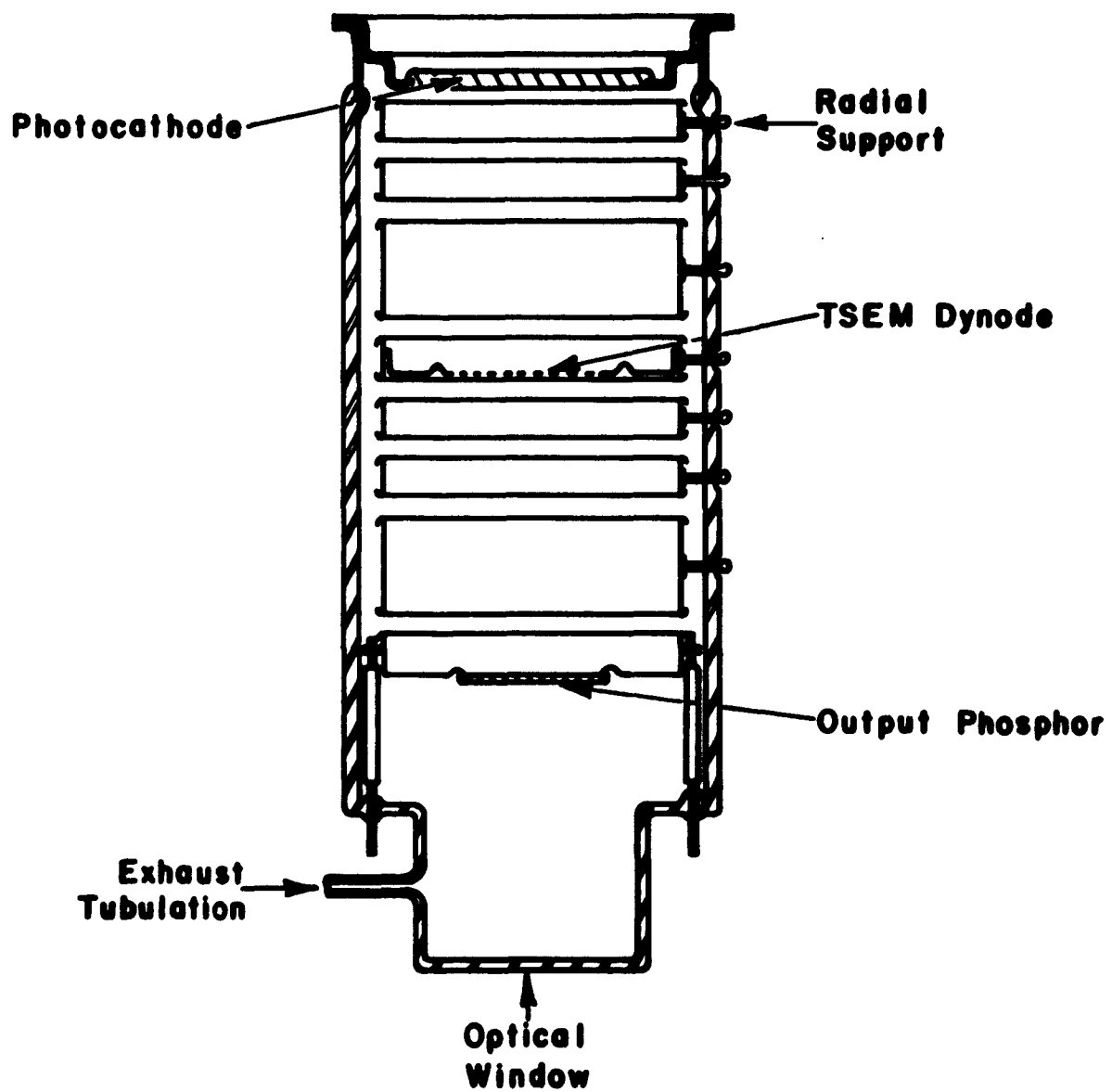**Output Phosphor**

Exhaust Tubulation

Optical Window

Figure 13.

of this experimental model was to permit:

(1) Direct visual observation of the imaging characteristics of the intensifier section.

(2) Evaluation of the problem of spurious background.

(3) Investigation of the problem of interaction by measurements of photo-cathode response and TSEM dynode gain.

A single mesh-supported, vacuum-evaporated KCl film was used together with a P-20 phosphor screen, at the respective design locations of the first and second TSEM dynodes. The reason for the mesh-supported film was to permit the use of a larger dynode, one inch as compared to the normal 3/4 inch diameter. This was considered an expedient measure until techniques for forming and applying large self-supporting TSEM films could be successfully developed. To minimize noise in the intensifier structure, antimony was pre-evaporated in a bell jar prior to assembly of the tube. Cesiation was effected during exhaust processing by means of internal cesium generators. The initial photoresponse of the Cs-Sb photo-cathode was 25 μA per lumen. The tube was operated at an interstage voltage of approximately 3 KV with an axial magnetic focusing field of 77 gauss. Magnification of the resultant image was 0.95. Under the described operating conditions, a resolution of 15.4 line pairs/mm was observed at the phosphor screen with no apparent S-distortion or image rotation. TSE dynode gain, as measured in the tube, was 4.1 at a primary voltage of 3.5 KV and 4.5 at 4.5 KV. Visual background emission was low at interstage voltages below 5 KV.

Based on the previously described design of the image intensifier section, image orthicon type tubes with two TSEM preamplifier stages were constructed as shown in Figure 14. A total of two tubes were fabricated, using mesh-supported, vacuum-evaporated KCl dynodes, one inch in diameter. The design of the tube permitted insertion of the target and dynodes just prior to the final step in tube construction, which consisted of heliarc welding the faceplate assembly to the front end. This was considered an important feature because it permitted minimum exposure to the atmosphere of both the thin film dynodes and target. In order to permit
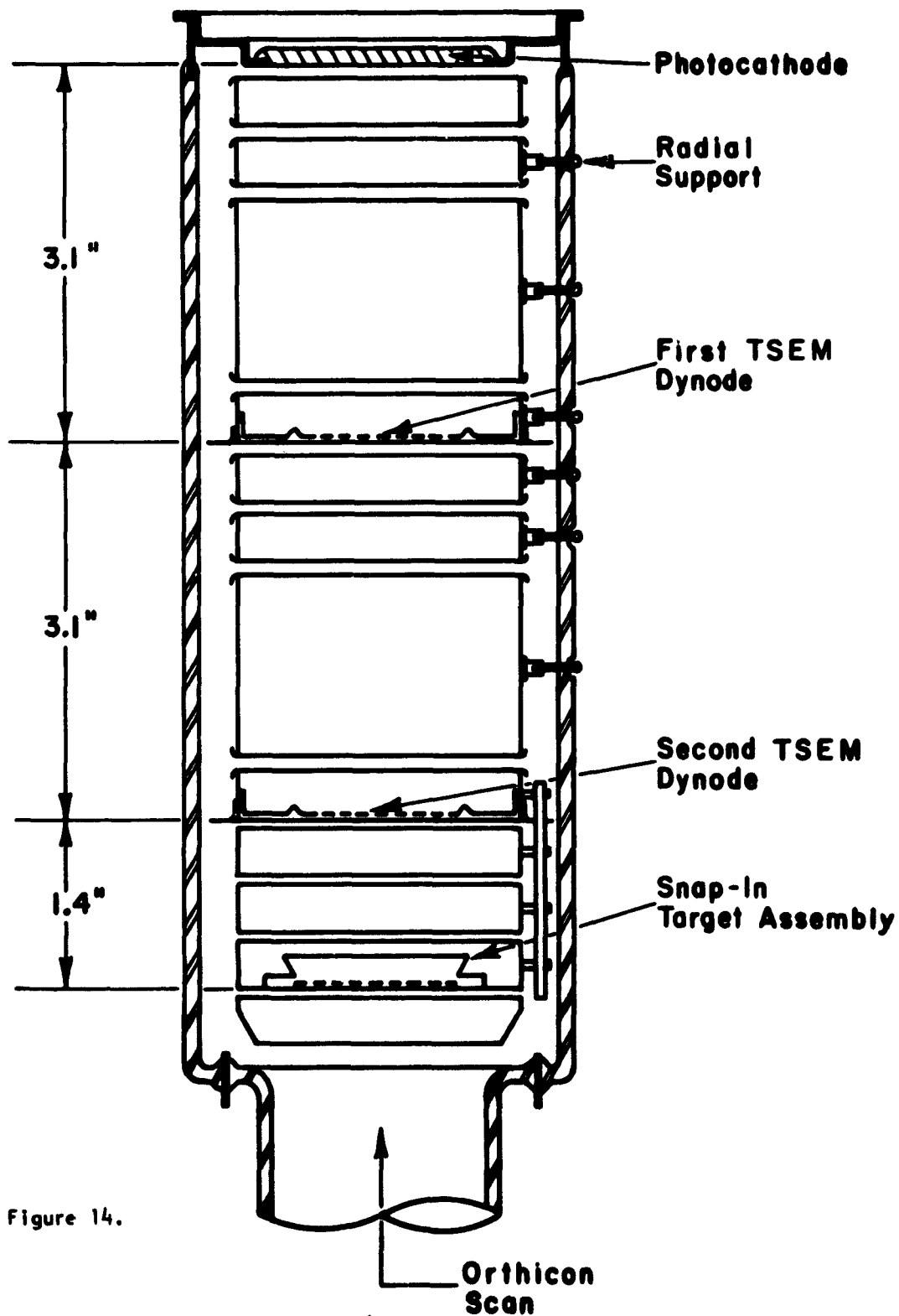
TSE INTENSIFIER-ORTHICON TUBE

Figure 14.

42

higher voltage operation in the final dynode to target stage of the intensifier section, the tubes employed a thin film aluminum oxide storage target. As in the image intensifier tube, a pre-evaporated antimony layer was used in the formation of the Cs-Sb photocathode. To realize an improved gain in the multiplier section a six dynode assembly was provided. Following a reduced temperature exhaust processing, the tubes were tipped-off with an attached Bayard-Alpert ionization gage. By subsequent operation of the ionization gage, it was possible to clean up residual gas accumulation in the tube. The performance of one of these tubes, TSE 2, is shown in the resolution versus photocathode illumination curve of Figure 15. This is compared with a representative TSE intensifier-orthicon tube, MC-7, employing two TSEM preamplifier dynodes, reported in Contract AF33(616)-3254[5]. Both tubes TSE-2 and MC-7, had a Cs-Sb photocathode with a sensitivity of approximately 20 μA per lumen. It should be pointed out that the resolution versus illumination curve for tube MC-7 had been adjusted for a photocathode sensitivity of 100 μA per lumen. It would appear, therefore, that performance of tube TSE-2 represents an approximate order of magnitude improvement over earlier tube MC-7. This includes, of course, the improvement due to an increase in dynode size from the earlier 3/4" diameter used in tube MC-7 to the 1" diameter in tube TSE-2.

Although an appreciable improvement in performance of the TSE intensifier-orthicon tubes was realized during the course of work on this contract, the theoretically predicted performance was still not attained. A fundamental limitation may be the aforementioned resolution limitation in the final TSEM dynode to target stage of the preamplifier section. As a result of these limitations and the concurrent successful application of the newly developed low density KCl film as an SEC target, in vidicon type tubes using direct beam readout, our efforts were redirected to the application of this film in a similar manner, in orthicon type tubes with return beam readout. Based on our experiences up to this point, it was expected that elimination of the pre-scanning beam dynodes and the use of a single high gain film as a combined preamplifier and target would improve our sensitivity and resolution capability.

SEC ORTHICON

Theoretical Performance

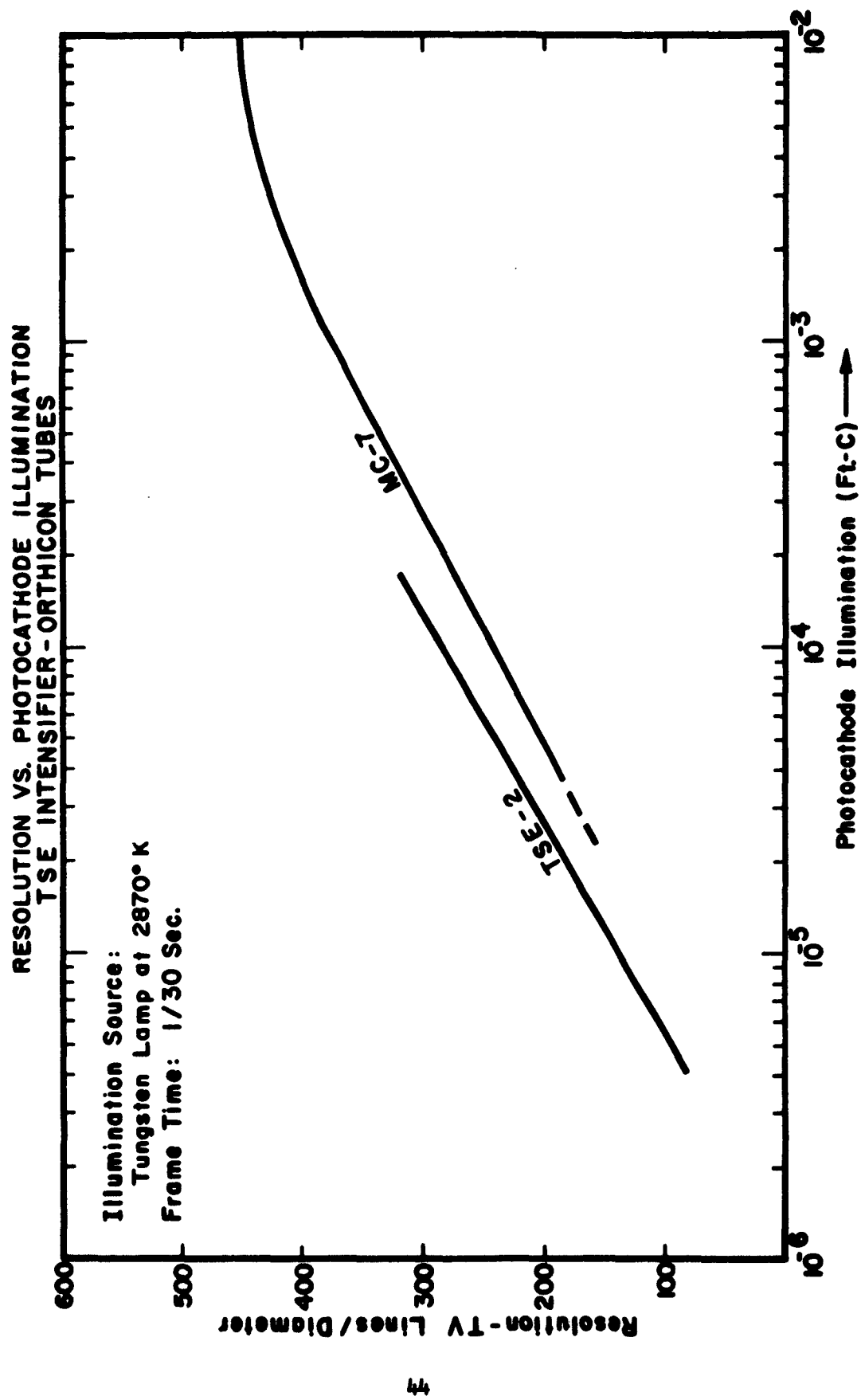As discussed in the previous section, the evaluation of the SEC target was

43

RESOLUTION VS. PHOTOCATHODE ILLUMINATION
TSE INTENSIFIER-ORTHICON TUBES

Illumination Source:
Tungsten Lamp at 2870° K
Frame Time: 1/30 Sec.

MC-1

TSE-2

Resolution-TV Lines/Diameter

600
500
400
300
200
100

10^{-6} 10^{-5} 10^{-4} 10^{-3} 10^{-2}

Photocathode Illumination (Ft-C) →

Figure 15.

44

conducted in vidicon type tubes using direct beam readout. With the realization
of a high gain target possessing the concomitant characteristics of fast response
and high resolution capability, the probability of extending the sensitivity by
the use of return beam readout arose. A comparison of return beam and direct beam
readout is therefore given in the following analysis[21]:

If the current leaving the photocathode of the tube is Is, then the noise
current associated with a system of bandwidth B is given by:

$$I_n = \sqrt{2\,e\,I_s\,B} = 5.65 \times 10^{-10} \sqrt{I_s B} \tag{31}$$

Similarly, the noise current associated with a scanning beam current, I_b, for a
return beam readout becomes:

$$I_n = 5.65 \times 10^{-10} \sqrt{I_b B} \tag{32}$$

The beam current is related to the photocathode current, I_s, and the target
current, I_T, in the following manner:

$$I_T = G\,I_s = M \cdot I_b \tag{33}$$

where M = modulation of the reading beam at the target

    G = target gain

The assumption is made that the total noise in the system can be obtained by
the square root of the sum of the squares of the noise contributions of the various
components. The signal-to-noise ratio of a camera tube with a high gain target
employing return beam scan in an 8 mc/sec. bandwidth system, assuming that the
return beam multiplier has sufficient gain to over-ride noise in the first amplifier
stage, can then be expressed by:

$$R_r = \frac{G\,I_s}{1.6 \times 10^{-6}\sqrt{G^2\,I_s + G\,I_s + \dfrac{G\,I_s}{M}}} \tag{34}$$

The signal-to-noise ratio for a tube with an identical image section but employing direct beam readout, an assumed value of 2×10^{-9} amperes noise current in the first stage of amplification, and an 8 mc/sec. bandwidth system, can be given by:

$$R_v = \frac{G \, I_s}{1.6 \times 10^{-6} \sqrt{G^2 \, I_s + G \, I_s + \dfrac{4 \times 10^{-18}}{2.56 \times 10^{-12}}}} \qquad (35)$$

Combining Equations (34) and (35) we obtain:

$$\left(\frac{R_r}{R_v}\right)^2 = \frac{G + 1 + \dfrac{1.56 \times 10^{-6}}{G \, I_s}}{G + 1 + \dfrac{1}{M}} \qquad (36)$$

where $\dfrac{R_r}{R_v}$ represents the advantage in signal to noise ratio of return beam relative to direct beam readout for a tube with a given image section embodying a target with gain, G.

The photocathode current, I_s, can be expressed by the following relation:

$$I_s = S \cdot A \cdot E \qquad (37)$$

where:

        S = photocathode sensitivity in amp per lumen

        A = photocathode area in sq. ft.

        E = photocathode illumination in ft-candles

Assuming: S = 150×10^{-6} amp per lumen

        A = .0064 ft.^{2} (35 mm diameter)

        Illumination source - tungsten lamp at 2870°K color temperature.

$$I_s = 9.6 \times 10^{-7} \, E \text{ is obtained.} \qquad (38)$$

Substituting this value of I_s in Equation (36) we obtain:

46

$$\left(\frac{R_r}{R_v}\right)^2 = \frac{G + 1 + \frac{1.62}{E \cdot G}}{G + 1 + \frac{1}{M}} \tag{39}$$

Shown in Figure 16 is a plot of R_r/R_v as a function of photocathode illumination, at various values of G with an assumed value $M = 0.1$. From this graph, the advantage of return beam relative to direct beam readout, in the region of lower light level, can be readily observed. For example, at a photocathode illumination of 10^{-8} ft-candles, and a target gain G = 100, the improvement in signal to noise ratio and consequently in resolution is in the order of 100. At higher light levels, the ratio R_r/R_v approaches unity.

It should be pointed out that the implied assumption in Equation (33) is a continuous adjustment of the readout beam to the varying photocathode illumination. If we assume, however, that the beam current will be kept constant at a selected value of photocathode illumination, Equation (39) becomes:

$$\left(\frac{R_r}{R_v}\right)^2 = \frac{G + 1 + \frac{1.62}{E \cdot G}}{G + 1 + \frac{E_o}{E \cdot M}} \tag{40}$$

where:

E_o = highlight photocathode illumination.

If $E_o = 10^{-4}$ ft-candles, then:

$$\left(\frac{R_r}{R_v}\right)^2 = \frac{G + 1 + \frac{1.62}{E \cdot G}}{G + 1 + \frac{10^{-4}}{E \cdot M}} \tag{41}$$

Referring to our previous example, at a photocathode illumination of 10^{-8} ft-candles and a target gain G = 100, the increase in signal to noise ratio now becomes 4. As before, at higher light levels, the ratio R_r/R_v approaches unity. Although the predicted improvement is much more conservative than that obtained

47

COMPARISON OF RETURN BEAM AND DIRECT BEAM READOUT

G=100

G=200

G=400

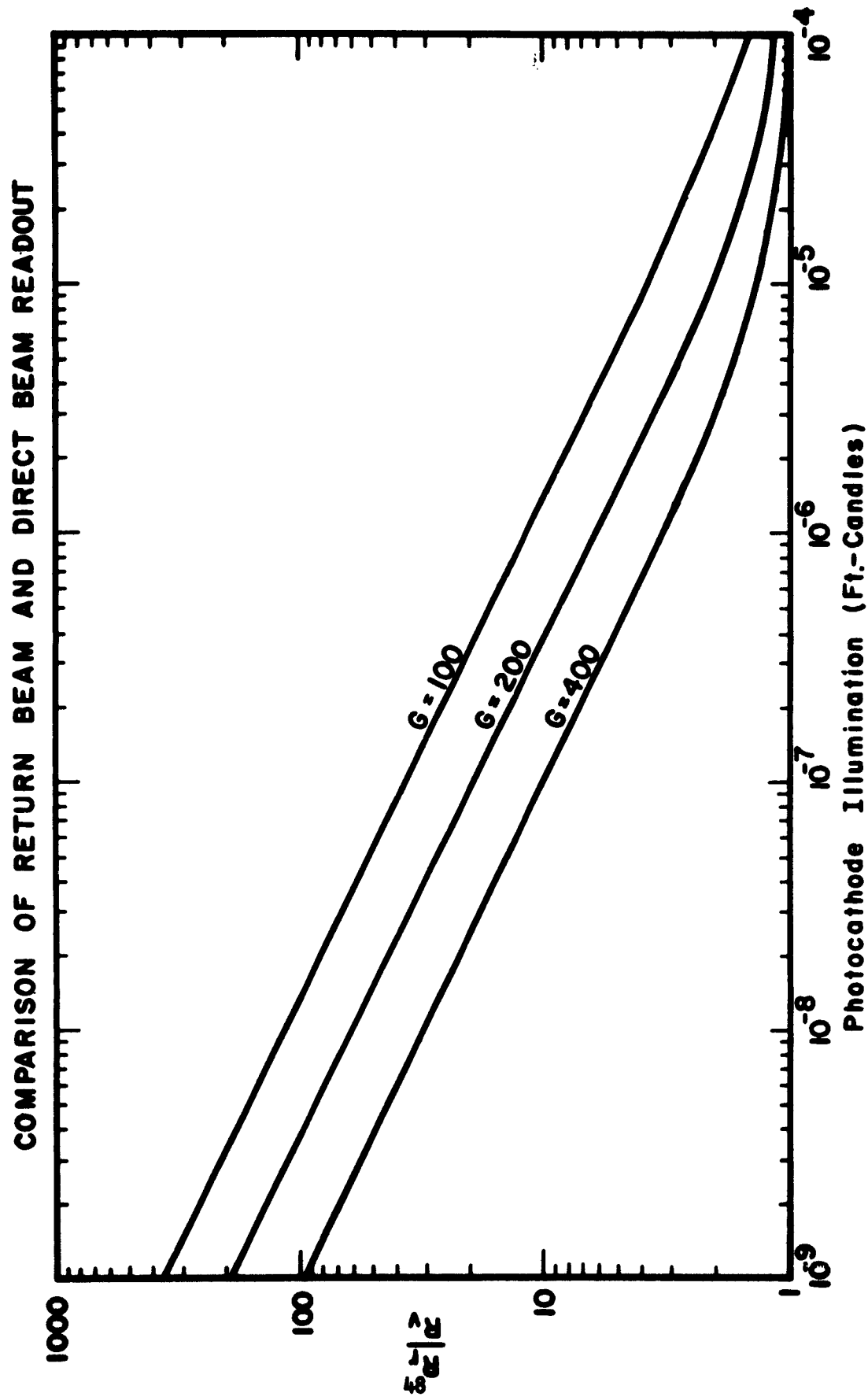Photocathode Illumination (Ft.-Candles)

Figure 16.

with the previous assumption, it still represents an appreciable advantage of return beam over direct beam readout.

This conclusion is further borne out by an analysis of resolution versus photocathode illumination performance. Shown in Figure 17 is a summary of performance characteristics of present state of the art television camera tubes compared with ideal photocathode noise limited performance. Curves I and V are theoretical resolution versus photocathode illumination plots at scene contrast ratios of 100% and 10% respectively, based on the idealized experiments of Coltman and Anderson[22]. Curves IV, VIII, and IX are based on measured data of a typical image orthicon with a thin film Al_2O_3 target (Westinghouse WL 22724), an electro-static Ebicon (Westinghouse WX 4772), and an electromagnetic Vidicon (WL 7325). Curve VII represents a theoretical electromagnetic Ebicon, predicted on the basis of a target gain of 100, photocathode sensitivity of 150 μA per lumen, photocathode diameter of 35 mm, and the aperture response of a conventional vidicon system. Interestingly, the actual performance of a typical Ebicon tube, shown in Curve VIII, is comparable to the predicted values, shown in Curve VII, at low light levels. The deviation from the predicted curve at higher light levels is probably due to the limitation imposed by electrostatic focusing in the image and scanning section of the actual tube. The Ebicon is closely related to the Uvicon described earlier with the exception of a visible light sensitive S-20 photocathode in the former. It employs direct beam readout of a high gain target, has an approximate photocathode diameter of 2" with minification to a target diameter of 5/8", and is electrostatically focused.

Curve II of Figure 17 is based on measured data of a typical single stage, magnetically focused intensifier-image orthicon (WX 4299) showing close approximation to the photocathode noise limited Curve I at the lower light levels. At the higher light levels, however, the actual curve falls away from the ideal curve. This is attributed primarily to the detail contrast degradation at the phosphor-photocathode intensifier stage in the image section of the tube. Curve II is representative of the performance achieved with tubes employing this method of image intensification. Although this method has led to the development of the most sensitive television camera tubes presently available, limitations arise from the inherent degradation in detail contrast due to the light flux-photoemissive coupling.
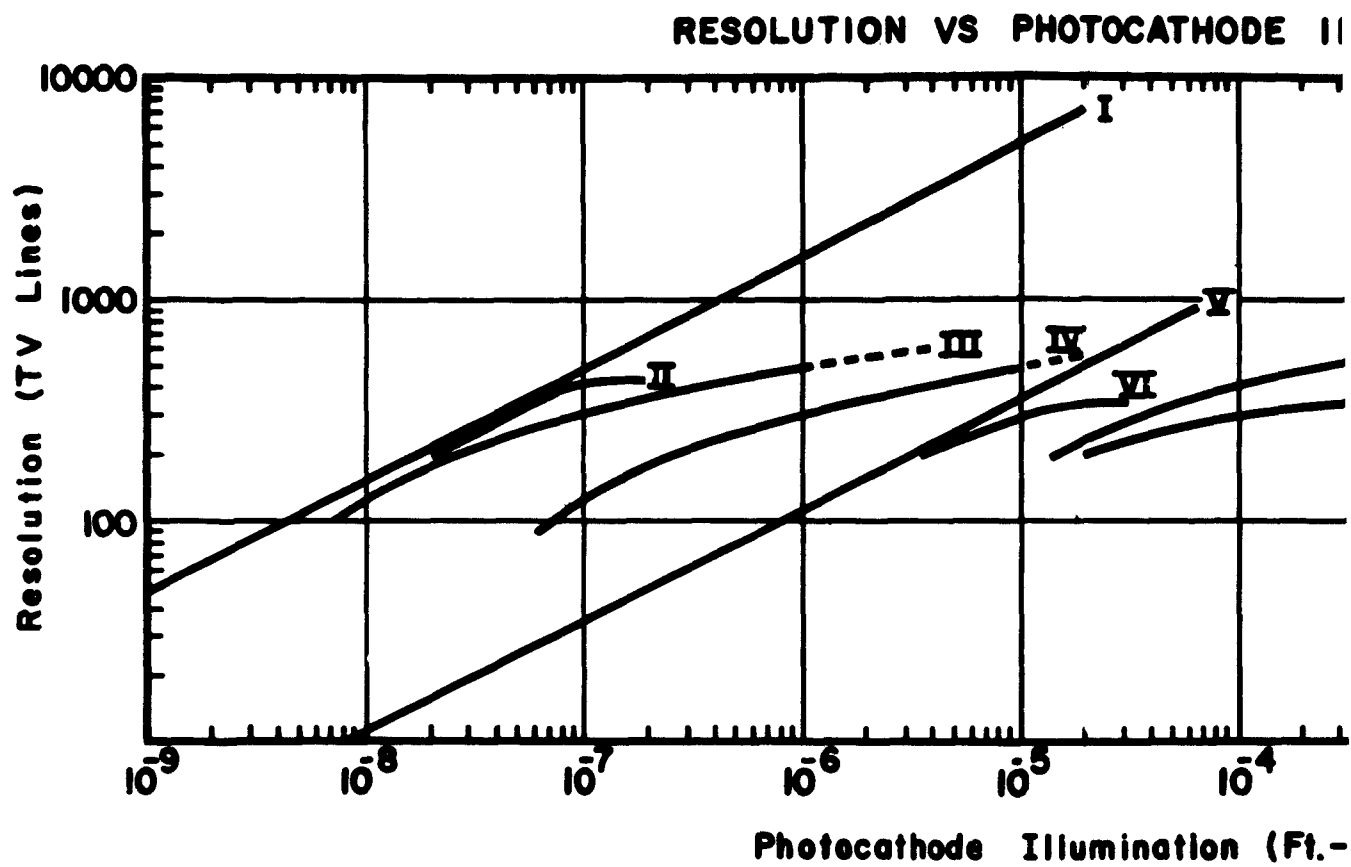
Figure 17.

50

RESOLUTION VS PHOTOCATHODE ILLUMINATION

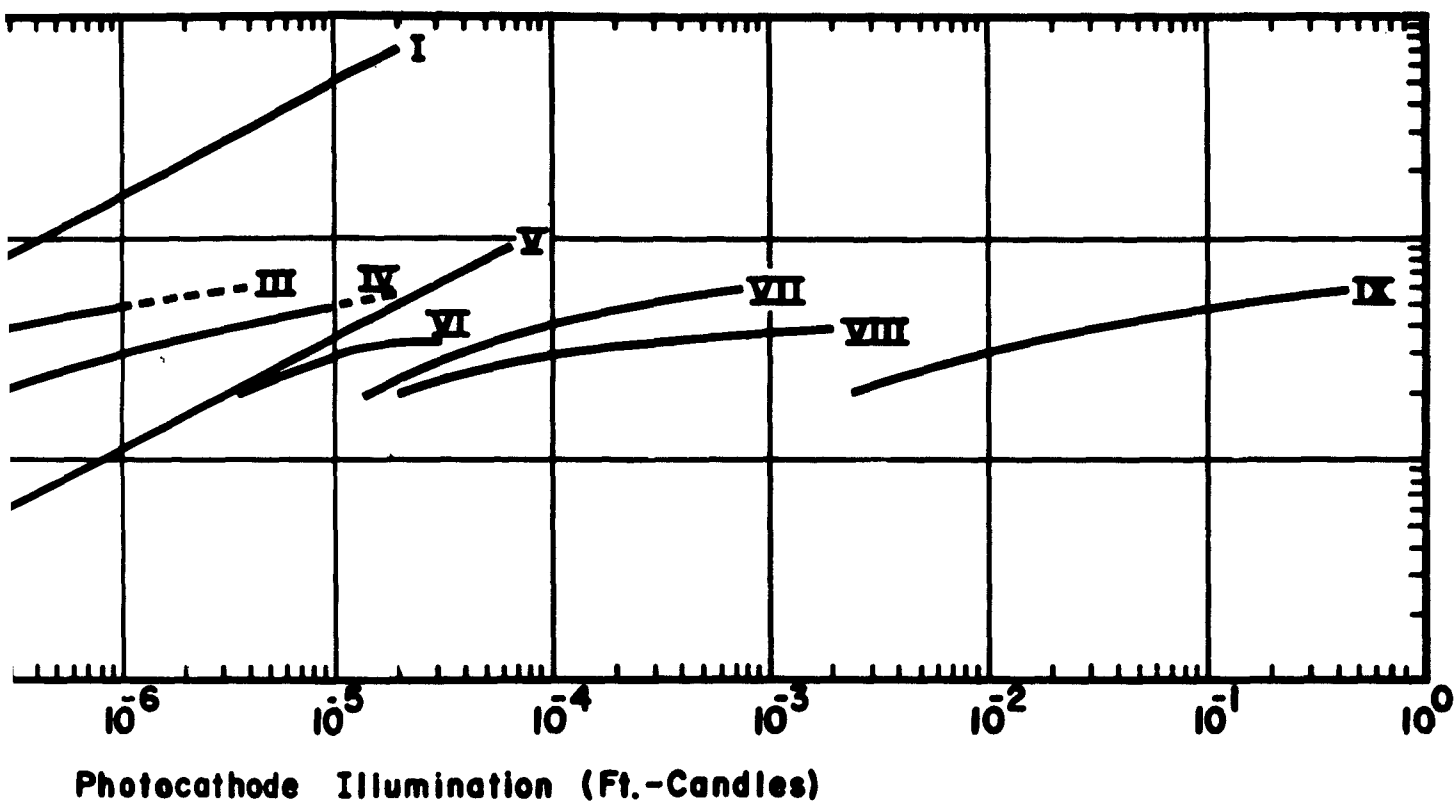Photocathode Illumination (Ft.-Candles)

Figure 17.

50

A critical examination of the performance curves shown in Figure 17 indicates the need for a camera tube which will approach the theoretical performance for scenes containing finer detail. Furthermore, since scene contrast ratios considerably less than 100% are encountered in real situations, there is need for a tube capable of providing useful images under such conditions. In addition, to permit imaging of a rapidly changing scene, one must impose the need for a tube with fast signal response. A promising solution to the problem of more closely approaching the performance of an ideal scanned optical amplifier would be the use of the high gain SEC target. This is suggested by observation of Curve IV of Figure 17, representing typical performance of an image orthicon with a thin film Al_2O_3 target. It is theorized that increasing the target gain of this tube ($G \cong 10$) by a factor of ten ($G \cong 100$), should result in a performance approaching that of ideal Curves I and V. This is shown in Curves III and VI of Figure 17 representing the theoretical performance of an SEC orthicon at scene contrast ratios of 100% and 10% respectively, based on a target gain of 100, a photocathode sensitivity of 150 μA/ lumen, and the aperture response of a camera system employing an image orthicon with an Al_2O_3 thin film target. The tube is magnetically focused and uses a return beam scan and multiplier section. As discussed previously, the use of a return beam and multiplier section is intended to improve performance at low light levels.

Although the predicted curves are based on the aperture response of a standard image orthicon with a thin film target, the combination of magnetic focusing and higher voltages in the image section employing an SEC target should result in improved limiting resolution. As defined, limiting resolution is achieved at signal levels under optimum imaging conditions of high scene brightness and 100% scene contrast ratio. A major factor determining this limitation is the image section focusing. To obtain a quantitative measure of improvement, consider the following relationship for a magnetically focused image section.

$$N = \frac{1}{2d} \frac{V}{V_o} \qquad \text{(line pairs per mm)} \qquad (42)$$

where: N = resolution limitation due to spread in initial emission velocity

d = photocathode to target spacing in mm.

V = potential difference between photocathode and target

V_o = most probable emission velocity of photoelectrons

51

If we assume that the magnetic field intensity and consequently the orbital period is the same in both the standard and high voltage image sections, then we must determine the conditions for equal electron time of flight. The time of flight is expressed by:

$$t = d \sqrt{\frac{2m}{V \cdot e}} \quad \text{for } V \gg V_o \tag{43}$$

The condition for equal time of flight is then given by:

$$\frac{d_2}{d_1} = \sqrt{\frac{V_2}{V_1}} \tag{44}$$

where: d_1 = photocathode to target spacing in the image section of an
            image orthicon.

          d_2 = photocathode to target spacing of an image section with the
            SEC target.

          V_1 = potential difference between photocathode and target of an
            image orthicon.

          V_2 = potential difference between photocathode and target of an image
            section with the SEC target.

Combining Equations (42) and (44) gives:

$$\frac{N_2}{N_1} = \sqrt{\frac{V_2}{V_1}}$$

where: N_2 = resolution limitation of an image section with the SEC target

          N_1 resolution limitation of image section of image orthicon

If we let: $V_2 = 8 \times 10^3$ volts

          $V_1 = 500$ volts

Then:

$$\frac{N_2}{N_1} = \sqrt{\frac{8 \times 10^3}{500}} = 4$$

We conclude that the image section with an SEC target should have a limiting resolution four times greater than that of the image section of a standard image

orthicon. As pointed out previously, however, the resolution capabilities imposed by other factors, such as the scanning beam optics, as well as that set by the associated equipment, combine to determine the overall resolution limitation of the system. Therefore, the actual effect of a higher resolution image section must be evaluated in the light of other contributing factors.

It is observed that Curves III and VI of Figure 17 approach their respective theoretical performance at the lower light levels. At the higher light levels, however, limiting resolution falls away from the ideal curves. This decrease in the slope of the high light level region is observed in all the tube performance curves shown in Figure 17. It is attributed to the focusing capability of each tube and the aperture limitation of the system. A comparison of theoretical Curve III with the measured data of a typical intensifier-orthicon in Curve II of Figure 17 shows an approximately equivalent performance at lower light levels and improved resolution at the higher light levels for the SEC orthicon.

Design and Construction

The design of the SEC orthicon is essentially a modification of the earlier TSE intensifier - orthicon structure, as shown in Figure 18. The design features of this tube include the following:

(1) Image section employing a low density KCl film as an SEC target.

(2) Photocathode to target spacing permitting single loop magnetic focusing with an axial magnetic field intensity of 75 - 85 gauss at an inter-electrode voltage of 7 - 8.5 KV.

(3) Front end loading of target, alkali generators, and antimony evaporator prior to final heliarc welding of the faceplate assembly. The purpose of this technique is to permit minimum exposure of these components, particularly the target, to the atmosphere.

(4) Control grid serving as a collector electrode for the target and also providing a uniform decelerating field to improve beam landing character-istics.

53

SEC ORTHICON

Electron Gun & Multiplier Assembly

Collector Grid

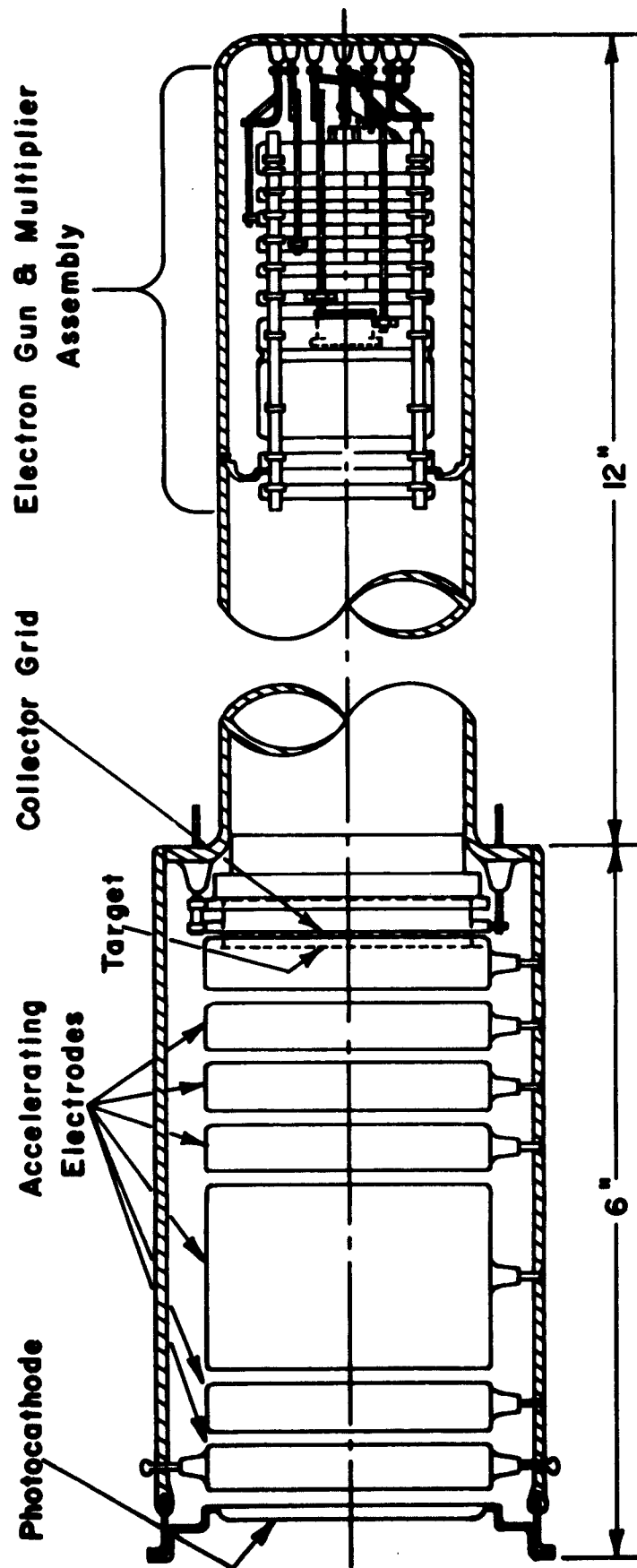Target

Accelerating Electrodes

Photocathode

12"

6"

Figure 18.

54

(5) Suppressor grid to prevent secondary electrons originating at the control grid from entering the multiplier structure.

(6) Image orthicon multiplier and gun assembly.

Redirection of our efforts occurred near the end of this contract period and consequently a limited time was available to construct and evaluate representative SEC orthicon tubes. A preliminary evaluation of experimental tubes constructed during this period established trends which should be of benefit in future investigations. In general, it was not difficult to process high sensitivity S-20 photocathodes within the structure, with sensitivities of 110 - 170 μA per lumen being achieved. Spurious background was low in most cases. Mesh supported low density KCl films, 1" in diameter, were used with no apparent difficulty encountered in tube.exhaust processing.

Since time did not permit complete measurement of these tubes, they were retained for further evaluation. Preliminary data on the most recent tubes indicates improved resolution capabilities in comparison with the best TSE intensifier-orthicon tubes as well as fast target response.

SECTION 5
CONCLUSION

Although an appreciable improvement in performance of the TSE intensifier-orthicon, employing transmission secondary electron emission films as pre-scanning beam amplifiers, was realized in the course of this contract, the theoretically predicted performance was not attained. This is attributed to the fundamental limitation imposed by the energy distribution of the transmission secondary electrons in the final dynode to target stage of the intensifier section. A possible further approach to this problem would be the use of a low density KCl dynode prior to an SEC target. Since the gain of the low density KCl dynode is in the order of 50 to 100, this combination should exhibit good resolution and a photoelectron utilization efficiency of essentially unity. In view of the theoretically predicted performance of an SEC orthicon, employing a single high gain target, with return beam readout, our efforts were redirected toward this more promising approach.

The measurements performed with the SEC target indicate that when employed in magnetically focused vidicon type camera tubes, it can be used to generate high quality television pictures (525 TV line resolution at standard frame rates) at photocathode illuminations of 10^{-4} to 10^{-3} ft-candles, comparable to the sensitivity of a conventional 5820 image orthicon. This sensitivity in readout is accompanied by extremely good target integration capabilities and fast response time.

In the case of direct beam readout, the average prebeam gain is 50 to 100 times less than the threshold gain for observing photoelectron scintillations. To extend the sensitivity of the tube to lower light levels, the SEC target was applied to an orthicon type camera tube with return beam readout and a signal multiplier section. The theoretical performance of such a tube should exceed that of an image orthicon with a thin film Al_2O_3 target and surpass the high light level performance of an intensifier-orthicon employing phosphor-photosurface intensifier stages.

PHOTOELECTRON UTILIZATION EFFICIENCY

A numerical example is given here in order to more clearly illustrate the effect of gain fluctuations on ϵ_2. Throughout this example a Poisson distribution in gain is assumed for the first stage while the remaining stages are assumed to be "noiseless". This corresponds to the assumption that each and every electron emitted by the first stage receives the same constant gain. Although such an approximation affords good accuracy only when the gain of the first stage is large, it is sufficiently accurate to demonstrate the effect of statistics on ϵ_2, even for relatively low mean gains. Such a treatment permits combining the mean gains of all cascaded stages except the first into one stage of constant gain.

Consider, then, an imaging device consisting of two stages, where the average gain of the first stage is $\overline{G}_1$ and the constant gain of the second stage is G_2. In this example G_o, the minimum gain required in order to record scintillations of single photoelectrons, is arbitrarily chosen at 240. The discrete probability that a photoelectron receives a gain, G, is plotted in Figure 19 for two values of $\overline{G}$, the average system gain $(\overline{G} = \overline{G}_1 G_2)$. For each of two values for $\overline{G}_1$, two values for G_2 are considered, one to typify the case where $\overline{G}$ is considerably less than G_o and the other to typify the situation that exists when $\overline{G}$ is only slightly less than or greater than, G_o. The data of Figure 19 can be applied to Equation (8) and ϵ_2 can be evaluated for each case.

Consider first the case where $\overline{G}$ is considerably less than G_o. In this case G_2 is adjusted so that for both values of $\overline{G}_1$, $\overline{G}$ equals 78. By using the scale at the top of Figure 19, then, it is obvious that the term, $P(G \geq G_o)$, of Equation (8) is essentially zero for both choices of $\overline{G}_1$. Thus, $\overline{G}'$, the average gain of those photoelectrons whose gain is less than G_o, is essentially $\overline{G}$ and from Equation (8), ϵ_2 has the value $\overline{G}/G_o$ or 0.32 for both choices of $\overline{G}_1$.

From Figure 19 it is clear that the only time the statistical fluctuations in gain become important is when $P(G \geq G_o)$ is non-zero, i.e., when $\overline{G}$ approaches or exceeds G_o. The values for G_2 associated with the scale at the bottom of Figure 19 have been chosen to yield a $\overline{G}$ exactly equal to G_o. The factors of Equation (8) and the resulting ϵ_2 are given in Table I. This data indicates that, for a fixed
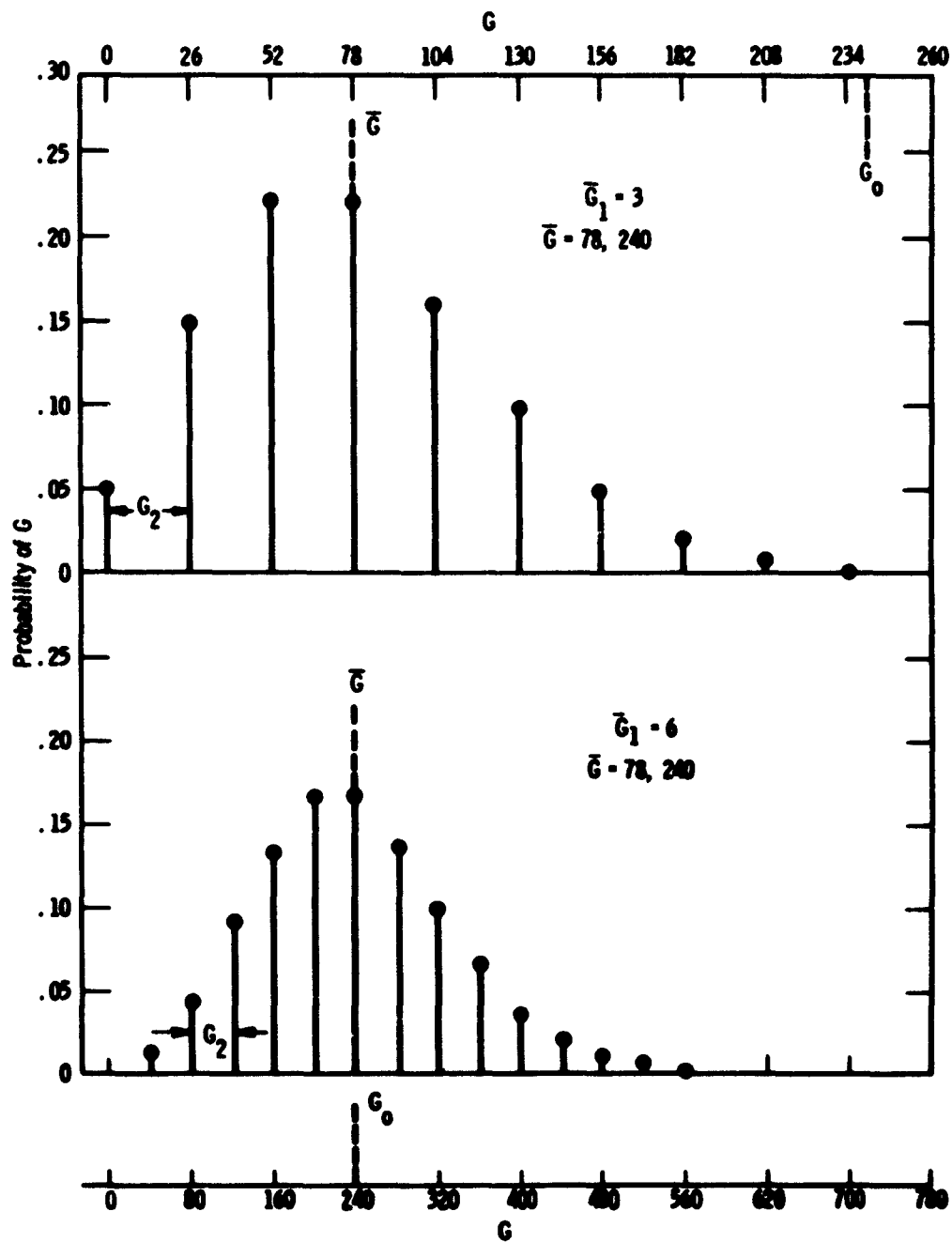
58

Figure 19. Poisson probability distribution of the gain of a photoelectron pulse

system gain, the utilization efficiency of photoelectrons is improved by including as much gain as possible into the first stage.

Also appearing in Table I, although not indicated in Figure 19, are similar computations for a $\bar{G}$ of 360 and 480 for the same choices of $\bar{G}_1$ and G_o.

<div align="center">

TABLE I

$\bar{G}$	$\bar{G}_1$	$P(G \geq G_o)$	$\bar{G}'$	ϵ_2
0.32 G_o	3	0	78	0.32
	6	0	78	0.32
1.0 G_o	3	0.57	108	0.77
	6	0.55	153	0.85
1.5 G_o	3	0.80	90	0.88
	6	0.84	148	0.94
2.0 G_o	3	0.80	120	0.90
	6	·0.94	125	0.97

</div>

BIBLIOGRAPHY

1. M. M. Wachtel, D. D. Doughty, A. E. Anderson, Advances in Electronics and Electron Physics, 12, 59, 1960.

2. Westinghouse Electric Corp., Electronic Tube Division, Final Report, Contract No. AF 33(600)-39403, Aeronautical Systems Division, Air Force Systems Command (To be released).

3. M. M. Wachtel, E. J. Sternglass, Phys. Rev. 100, 1238, 1955.

4. M. M. Wachtel, E. J. Sternglass, Bull. Am. Phys. Soc. 1, 38, 1956.

5. J. A. Hall, H. Shabanowitz, Westinghouse Electric Corp., Electronic Tube Division, Contract No. AF 33(616)-3254, Aeronautical Research Laboratory Report ARL 154, Dec. 1961.

6. M. M. Wachtel, Westinghouse Research Laboratories, Final Report, Contract No. DA-44-009-ENG-3492, Engineer Research and Development Laboratory, Ft. Belvoir, Va; May 21, 1959.

7. M. M. Wachtel, A. E. Anderson, Westinghouse Research Laboratories, Final Report, Dept. of Terrestrial Magnetism, Carnegie Institution of Washington.

8. A. Rose, Advances in Electronics, 1, 131, 1948.

9. A. H. Sommer, Rev. Scient, Instr. 26, 725, 1955.

10. D. J. Gibbons, Advances in Electronics and Electron Physics, 12, 203, 1960.

11. H. Richard Groo, Proceedings of the Image Intensifier Symp., Fort Belvoir, Va., 55, 1961.

12. W. J. Wilcock, D. L. Emberson and B. Weekley, IRE Trans. PGNS, NS-7, 126, 1960.

13. R. G. Stoudenheimer, T. C. Moor, H. L. Palmer, IRE Trans. PGNS, NS-7, 136, 1960.

14. J. R. Waters, G. T. Reynolds, D. B. Scarl and R. A. Zdanis, Proc. of the Eighth Scintillation and Semiconductor Counter Symposium, Washington, D.C., 1962 (To be published)

15. G. W. Goetze, Proc. of the Second Symp. on Photoelectronic Image Devices, London, 1961. (To be published)

16. R. J. Schneeberger, G. Skorinko, D. D. Doughty and W. A. Feibelman, Proc. of the Second Symp. on Photoelectric Image Devices, London, 1961. (To be published)

17. S. Taylor, Advances in Electronics 12, 263, 1960.

18. J. Dresner, RCA Review, 22, 305, 1961.

19. W. Baum, Trans. Int. Astr. Un., 9, 676, 1955.

20. G. Skorinko, D. D. Doughty, W. A. Feibelman and R. J. Schneeberger, Westinghouse Research Report 912-J902-R1, 1961.

21. J. Lempert, G. Klotzbaugh, Westinghouse Research Laboratories, Fourth Quarterly Report, Contract No. DA 36-039 sc-87397, U. S. Army Signal Research and Development Laboratory, March 20, 1962.

22. J. W. Coltman, A. E. Anderson, Proc. IRE, 48, 858, 1960.

Cys	ACTIVITIES AT WPAFB
1	ASAPR (OTS Review)
1	ASAPR (Library)
3	ASAPT
2	ASRMRS-1
6	ASRMET-2

OTHER DEPARTMENT
OF DEFENSE ACTIVITIES

Air Force

Cys	
1	RADC (RCSGA) Attn: Mr. Kesselman Griffiss AFB NY
1	AFSWC (SWOI) Kirtland AFB NMex
1	AFMTC Attn: AFMTC Tech. Library MU-135 Patrick AFB Fla
1	RADC Attn: RCSSL-1, Documents Library Griffiss AFB NY
1	AFGC (PGTRI) Eglin AFB Fla
1	BSD (WDTG) AF Unit Post Office Los Angeles 45 Calif
1	AFMDC (MDGRT-1) Holloman AFB NMex
1	ESD L G Hanscom Fld Bedford Mass
1	SSD AF Unit Post Office Los Angelas 45 Calif

Cys	Air Force (Cont'd)
1	Electro-Optical Surveillance Station P. O. Box 314 Cloudcroft, New Mexico

Navy

Cys	
1	Chief Bureau of Ships Attn: Mrs. F. A. Darne, Code 691A Washington 25, D. C.
1	Chief Naval Research Laboratory Bldg. 33, Room 105 Washington 25, D. C.
1	Naval Ordnance Test Station Attn: Mr. J. Rughe 1207 Michelson Laboratory China Lake, California
1	Naval Ordnance Laboratory Attn: Mr. M. P. Nordseth Corona, California

Army

Cys	
1	Commanding General U. S. Army Engineer Research and Development Laboratory Attn: Warfare Vision Branch Ft. Belvoir, Virginia
1	Commanding Officer U. S. Army Signal Research Development Laboratory Attn: SELRA-PRG Ft. Monmouth, New Jersey
1	Commanding Officer U. S. Army Electronic Proving Ground Attn: Combat Area Surveillance Department Ft. Huachuca, Arizona

ASD-TDR-63-84

Cys	Army (Cont'd)
1	Commanding General Frankford Arsenal Attn: Dr. M. L. Chalow, 1130 Philadelphia 37, Pennsylvania

OTHER US GOVERNMENT AGENCIES

Cys	
30	ASTIA (TIPCR) Arlington Hall Stn Arlington 12 Va
4	Advisory Group on Electronic Devices Attn: Secretary, Working Group on Special Devices 346 Broadway, 8th Floor New York 13, New York

NON-GOVERNMENT INDIVIDUALS
AND ORGANIZATIONS

Cys	
1	The Rand Corporation Attn: Librarian 1700 Main Street Santa Monica, California
3	Radio Corporation of America Attn: Mr. G. W. Kimball 224 North Wilkinson Street Dayton 2, Ohio
3	Westinghouse Electric Corporation Attn: Mr. John Basista 32 North Main Street Dayton 2, Ohio
1	Westinghouse Electric Corporation Electronic Tube Division Attn: Mr. Harry Shabanowitz P. O. Box 284 Elmira, New York
1	General Electric Company Cathode Ray Tube Department Attn: Dr. P. Wargo Electronics Park Syracuse, New York

Cys	NON-GOVERNMENT INDIVIDUALS AND ORGANIZATIONS (Cont'd)
1	University of Minnesota Institute of Technology Department of Electrical Engineering Attn: Dr. W. G. Shepherd Minneapolis, Minnesota
1	Massachusetts Institute of Technology Lincoln Laboratory Attn: Library P. O. Box 73 Lexington 73, Massachusetts
1	ITT Federal Laboratories 3301 Wayne Trace Fort Wayne 1, Indiana Attn: Reports Librarian
1	Hallamore Electronics Division 714 North Brookhurst Street Anaheim, California Attn: R. Van Decael
22	Office of Technical Services Department of Commerce Washington 25, D. C.

ASD-TDR-63-84